

Pharmacokinetics and dosimetry in intraperitoneal radioimmunotherapy with ^{211}At

Elin Cederkrantz

Department of Radiation Physics
Institute of Clinical Sciences
Sahlgrenska Academy at University of Gothenburg



UNIVERSITY OF GOTHENBURG

Gothenburg 2014

Pharmacokinetics and dosimetry in intraperitoneal radioimmunotherapy with
211At

© Elin Cederkrantz 2014
elin.cederkrantz@radfys.gu.se

ISBN 978-91-628-8891-6

E-publication: <http://hdl.handle.net/2077/34850>

Printed in Gothenburg, Sweden 2014
Ale Tryckteam

To my family with love

*"Some people say little girls should be seen and not heard. But I say...
Oh Bondage, up yours!"*

Poly Styrene, X-ray Specs, 1977

"Det går inte att bromsa sig ur en uppförsbacke."

Sally Santesson (Ulf Malmros)

Pharmacokinetics and dosimetry in intraperitoneal radioimmunotherapy with ^{211}At

Elin Cederkrantz

Department of Radiation Physics, Institute of Clinical Sciences
Sahlgrenska Academy at University of Gothenburg, Göteborg, Sweden

ABSTRACT

The prognosis for patients diagnosed with disseminated cancer is often poor. Radioimmunotherapy (RIT) is a new approach to treat disseminated disease. The aim is to target tumor cells with monoclonal antibodies (mAbs) labeled with radionuclides which release cytotoxic particle radiation upon decay. The radionuclide ^{211}At , with half-life 7.21h, is an interesting candidate for RIT. It emits an α -particle which leaves a short, dense ionization track along its path. The range of the α -particle ($<100\ \mu\text{m}$) corresponds to a few cell diameters. Thus, with ^{211}At in combination with a tumor-specific mAb, a high level of irradiation may be achieved in very small tumors, while, at the same time, the surrounding tissue is spared.

In this thesis, the pharmacokinetics of intraperitoneal (IP) ^{211}At -MX35 F(ab')₂ for ovarian cancer was investigated in 12 patients partaking in a phase I study. The *in vivo* distribution was monitored by sampling of bodily fluids and gamma camera imaging. Absorbed doses to normal organs and tissues were estimated. The peritoneum was subjected to the highest absorbed dose of all investigated tissues after the amendment of a thyroid blocking agent. The radiation tolerance of the peritoneum was unknown and was therefore studied in an animal model. The absorbed doses associated with therapeutic activity levels were found to be well tolerated in a short term perspective.

Exposure to α -particles is however associated with a high risk for cancer induction. The ICRP recommends a radiation weighting factor 20 for α -particles. The effective dose provides a tool for estimating the risk associated with a procedure involving irradiation. It was estimated to $< 2\ \text{Sv}$ for a general patient undergoing IP ^{211}At -RIT with 300 MBq in 1.5 L icodextrin.

Keywords: astatine-211, radioimmunotherapy, alpha-emitter, ovarian cancer, MX35, pharmacokinetics, dosimetry, effective dose

ISBN: 978-91-628-8891-6

E-publication: <http://hdl.handle.net/2077/34850>

LIST OF PAPERS

This thesis is based on the following studies, referred to in the text by their Roman numerals.

- I. Andersson H, Cederkrantz E, Bäck T, Divgi C, Elgqvist J, Himmelman J, Horvath G, Jacobsson L, Jensen H, Lindegren S, Palm S, Hultborn R.
Intraperitoneal α -particle radioimmunotherapy of ovarian cancer patients: pharmacokinetics and dosimetry of ^{211}At -MX35 F(ab')₂ – A phase I study.
J Nucl Med 2009; 50(7):1153-1160.
- II. Cederkrantz E, Angenete E, Bäck T, Falk P, Haraldsson B, Ivarsson M-L, Jensen H, Lindegren S, Hultborn R, Jacobsson L.
Evaluation of effects on the peritoneum after intraperitoneal α -radioimmunotherapy with ^{211}At .
Cancer Biother Radiopharm 2012; 27(6):353-364.
- III. Cederkrantz E, Bäck T, Lindegren S, Palm S, Magnander T, Bernhardt P, Andersson H, Jensen H, Hultborn R, Jacobsson L, Albertsson P.
Effective dose of intraperitoneal α -radioimmunotherapy with ^{211}At for ovarian cancer patients.
Manuscript.

TABLE OF CONTENTS

ABBREVIATIONS	X
1 INTRODUCTION	1
1.1 Internal radiation therapy	1
1.2 Radioimmunotherapy	2
1.2.1 The target	2
1.2.2 Antibodies	4
1.2.3 Radionuclides	5
1.3 The therapeutic window	9
1.4 Ovarian Cancer	11
2 AIM	15
3 PATIENTS AND METHODS	17
3.1 Clinical study	17
3.1.1 Patients	17
3.1.2 Clinical protocol	17
3.2 Animal study	18
3.2.1 Animals	18
3.2.2 Short term experiments	18
3.2.3 Long term experiment	21
3.3 Radionuclides	21
3.3.1 ^{211}At	21
3.3.2 ^{125}I	24
3.3.3 ^{51}Cr	24
3.3.4 $^{99\text{m}}\text{Tc}$	24
3.4 Monoclonal antibodies	25
3.4.1 MX35	25
3.4.2 Trastuzumab	25
3.5 Radiolabeling with ^{211}At	26
3.6 Radioactivity measurements	27

3.7 Gamma camera imaging	27
4 RADIATION DOSIMETRY	29
5 RESULTS	33
5.1 Clinical results.....	33
5.1.1 Pharmacokinetics.....	33
5.1.2 Dosimetry	38
5.2 Preclinical results	41
6 DISCUSSION AND CONCLUSIONS.....	43
7 FUTURE PERSPECTIVES	47
ACKNOWLEDGEMENT	49
REFERENCES	51

ABBREVIATIONS

Bq	Becquerel, 1 Bq = 1 nuclear transition per second.
CA-125	Cancer antigen 125
CT	Computed tomography
DNA	Deoxyribonucleic acid
DTPA	Diethylene triamine pentaacetic acid
EDTA	Ethylene triamine tetraacetic acid
FDA	Food and Drug Administration, USA
Gy	Gray, 1 Gy = 1 J/kg
HAMA	Human antimouse antibody
HER2	Human epidermal growth factor receptor 2
ICRP	International Commission on Radiological Protection
IP	Intraperitoneal
IRF	Immunoreactive fraction
IRT	Internal radiation therapy
IV	Intravenous
J	Joule, 1 J = 1 kg m ² s ⁻²
KClO ₄	Potassium perchlorate
kg	Kilogram, 1 kg = 1000 g
KI	Potassium iodide
LET	Linear energy transfer

mAb	Monoclonal antibody
MIRD	Committee on medical internal radiation dose
NaPi2b	Sodium-dependent phosphate transport protein 2b
NIS	N-iodosuccinimide
OSEM	Ordered subset expectation maximum
RBE	Relative biologic effect
RIT	Radioimmunotherapy
SAF	Specific absorbed fraction
SI	Standard international (unit)
SPECT	Single photon emission computed tomography

1 INTRODUCTION

The papers presented in this thesis are part of a translational research project with the aim to develop effective and safe radioimmunotherapy against cancer. Basic research in immunology, oncology, radiation physics, nuclear physics, radiochemistry, radiobiology, and computational science paved the way for this work. The focus of this thesis was to evaluate pharmacokinetics and dosimetry of a radioimmunoconjugate specifically targeting epithelial ovarian cancer with the aim to determine feasibility and safety of intraperitoneal (IP) radioimmunotherapy (RIT) with the α -emitter ^{211}At . In two of the three papers (I&III), results from a phase I study are presented. In paper II, the radiation tolerance of the peritoneum was investigated in an animal study.

1.1 Internal radiation therapy

Internal radiation therapy (IRT) is one of several alternatives for cancer therapy under development. For a few malignancies IRT is an effective stand-alone therapy, but best results are in most situations achieved by a combination of different therapeutic regimens; surgery, chemotherapy and external radiotherapy being predominant. The principle for IRT is to achieve local irradiation of malignant tissue by administration of a radioactive substance which accumulates in the target tissue. The purpose of the irradiation is to induce irreparable damage to the cancer cells so that they are killed or at least stop proliferating. IRT can be of particular importance for malignancies with multiple small targets, i.e. disseminated disease, and for hematologic diseases; conditions with the common characteristic that the cancer cells are difficult to locate or isolate for treatment with surgery or external radiotherapy. IRT is however not limited to such applications. For example, radioiodine (^{131}I) against hyperthyroidism and certain thyroid cancers is a well-established IRT which has been practiced since the 1940's [1]. In radioiodine therapy, the normal function of thyroid tissue, to accumulate iodine, is taken advantage of. The radioactive iodine isotope ^{131}I has exactly the same biochemical properties as stable iodine and is therefore spontaneously and effectively accumulated in thyroid tissue which gives a high ratio between the level of irradiation of the thyroid and the rest of the body. For most cancers, however, it is not possible to achieve specific targeting with a free radionuclide; a vector to carry the radionuclide to the target is required. This "magic bullet" concept was envisioned by Paul Ehrlich over a century ago [2]. He hypothesized that if a substance that

specifically binds to a disease-causing tissue could be found, it could be utilized for selective delivery of a toxin to said tissue. By researchers following in his footsteps, a vast selection of molecules have since been investigated, e.g. peptides, lipids, colloids, and antibodies for targeting of different malignancies. The terminology “magic bullet” and “targeting” is however somewhat misleading as there is no magic or intelligence involved in the processes concerned. It is just a matter of finding molecule A with high and specific affinity for target B. A will then spontaneously accumulate in B by chemical binding as it happens to pass nearby or through B while following the normal circulation in the body.

1.2 Radioimmunotherapy

In this thesis, a monoclonal antibody (mAb) was used for targeting of cancer cells, a branch of IRT called radioimmunotherapy (RIT). The binding of a mAb to an antigen may have a standalone therapeutic effect by alerting the immune system to reject and destroy the cancer cells (immunotherapy) [3, 4]. In RIT, a radionuclide is conjugated to the mAb and the therapeutic effect is achieved or enhanced by localized irradiation of the targeted tumor cells. RIT has been in clinical practice for approximately a decade. ^{90}Y -ibritumomab tiuxetan (Zevalin) targeting the antigen CD20 found on the surface of B-cells was approved by the Food and Drug Administration (FDA), USA, in 2002 for treatment of lymphoma [5]. ^{131}I -tositumomab (Bexxar), approved in 2003, targets the same antigen and was also used for treatment of lymphoma [6]. The withdrawal of Bexxar due to declining sales was however recently announced in spite of convincing clinical data. Tough competition and a dependence on foreign radionuclide production were important contributing factors to the failure to gain market shares in the US. Nevertheless, research to develop RIT against CD20-diseases, epithelial cancers, as well as some solid tumors is currently conducted across the globe [7-11]. The challenge is to optimize the combination of vector, radionuclide and administration route for the specific tumor type so that the radiation reaches the target with minimal irradiation of other tissues. The efficacy of RIT is dependent on many factors which will be addressed in the following sections.

1.2.1 The target

Tumor cells are characterized by their differences from normal cells. Alterations in the expression of antigens on the cell surface, particularly overexpression, can be utilized for specific targeting with mAbs. The first step in the development of RIT against a specific type of cancer is thus to identify a suitable antigen to target the therapy against. The antigen should be

highly and homogeneously expressed by tumor cells and ideally not be expressed at all by normal cells. It should not be shedded from the cancer cells, because shedded antigens may form complexes with mAbs in circulation, thus reducing the number of mAbs eligible for reaching the target. In addition, the antigen should stay in its position on the cell surface after binding an antibody for a sufficient amount of time so that the attached radionuclide has time to decay and release the cytotoxic radiation at the intended location. If internalization of the antigen along with the radioimmunoconjugate can be expected to promote accumulation of the radionuclide within the tumor cells, that may be preferred to a stable position on the cell surface.

Identification of targets for immunotherapy and RIT is a major field of study. Just to mention a few, CD19, CD22, CD25, CD37, CD45, CD52 and HLA class II have all been suggested as target antigens for different types of lymphomas and leukemias in addition to CD20 mentioned above [12, 13]. Potential targets for ovarian cancer therapy are, e.g., folate receptor alpha [14-16], sodium-dependent phosphate transport protein 2b (NaPi2b) [17-19], and, although primarily associated with breast cancer, human epidermal growth factor 2 (HER2) [20, 21]. It should be noted that (for instance) ovarian cancer is a family name for many different histological ovarian cancer subtypes with different antigen expression profiles and that a specific antigen may not be expressed by all subtypes. The amount of antigen per cell may also vary between cells of a certain subtype. It should also be realized that antigens are seldom exclusively expressed by tumor cells and that the search for potential therapeutic targets is often concerned with finding antigens with a good ratio of expression in malignant versus normal tissue. Research dedicated to characterizing and quantifying the antigen expression of different cancers and normal tissues is therefore of uttermost importance for the development of targeted therapies.

Another prerequisite for achieving successful RIT is that all tumor cells must be accessible for the targeting mAbs or at least within range of the radiation. The tumor growth pattern, vascularization and location may thus be factors influencing the possibility to treat the disease. Access to tumor cells in various locations can be promoted by choosing a suitable administration route. Accessibility is however a major reason for why RIT is best suited for tumors of small dimensions. Large solid tumors are often associated with compromised vascularization and high interstitial pressure which may inhibit diffusion of the therapeutic agent into the tumor tissue, with incomplete irradiation as a consequence. If a radionuclide with long-ranged particle emissions is used, cross-fire irradiation can compensate for inhomogeneous

intratumoral accumulation to a certain extent. The choice of radionuclide will be further discussed below.

1.2.2 Antibodies

Antibodies are large Y-shaped proteins of about 150 kDa belonging to the immunoglobulin (Ig) superfamily. An antibody comprises two heavy and two light identical polypeptide chains. Depending on the characteristics of the heavy chains antibodies differentiate into five isotypes: IgA, IgD, IgE, IgG and IgM, with different biologic functions. The IgG isotype is involved in pathogen immunity and is the main candidate for targeting applications. Their primary function is to identify and neutralize objects foreign to the host, e.g., bacteria, viruses or cancerous cells. They do so by attaching to the target which may have a direct effect, e.g., blocking proliferative functions or induction of apoptosis, or an indirect effect, i.e., alerting the immune system to attack the pathogen.

Antibodies are produced by B-cells upon exposure of an antigen. Any foreign substance with the ability to induce an immune response can be defined as an antigen. In RIT, the antigen is often a protein or large carbohydrate on the tumor cell surface. An antigen may have several epitopes, i.e., binding sites for antibodies, by which B-cells can be activated respectively. Activated B-cells proliferate, i.e., generate identical B-cell clones, and produce antibodies against specific epitopes. Hence, a normal immune response against a certain antigen is a concerto of polyclonal antibodies released into the blood stream. Experiments with polyclonal antibodies were conducted as early as the late 19th century. Behring and Kitasato were first to describe how serum from an animal infected with diphtheria or tetanus could cure other infected animals and protect healthy animals from infection [22].

Monoclonal antibodies are, as opposed to polyclonal antibodies, derived from identical B-cell clones and they are specific for one particular epitope on an antigen. The specificity of mAbs is a highly valued characteristic in diagnostic as well as therapeutic applications. A method for production of mAbs *in vitro* was reported by Köhler and Milstein in 1975 [23]. By fusion of a B-cell with a melanoma cell, antibody-producing hybridoma cells were derived, which could be cultured and harvested for mAbs indefinitely. The discovery made mAbs conveniently available in large quantities, which strongly promoted further development of immunotargeting techniques. A mAb with high affinity for a tumor cell antigen, and no specific binding to other tissues is ideal for RIT. Screening for such mAbs is continuously conducted for various applications.

MAbs have two identical paratopes, i.e., antigen-binding sites, located at the tips of the Y-shape respectively. The paratope gives the antibody its specificity and is exclusive for each kind of antibody. MAbs can be fragmented with preserved specificity by exposure to enzymes. Papain cleaves an antibody at the intersection of the Y-shape, resulting in two antigen-binding fragments (Fab) and one crystallizing fragment (Fc) of about 50 kDa respectively [24]. If instead pepsin [25, 26] or IdeS [27] is applied, the antibody is cleaved below the hinge region, resulting in a divalent antigen-binding fragment ($F(ab')_2$) of approximately 115 kDa, which can be further fragmented into two Fab's by mild reduction [28]. Removal of the Fc region may be beneficial in some situations, e.g., if immunoreactivity of the Fc region interferes or competes with antigen targeting. A reduced molecular size may also lead to faster biokinetics and better diffusive penetration of the target tissue [29]. Furthermore, a fragmented antibody has a shorter biologic half-life, i.e., the fraction which does not find or bind to the target is rapidly excreted. With different biochemical techniques even smaller fragments can be derived, e.g., scFv, VHH/VH, diabodies and minibodies, none of which have however yet been approved for clinical use [30, 31].

MAbs used for targeting applications are often of animal origin, the most common being murine. If the humoral immune system recognizes this, production of human anti-mouse antibodies (HAMA), or equivalent, is initiated [32], the presence of which may interfere and disrupt a therapeutic or diagnostic procedure. HAMA may be present without previous treatment with murine antibodies, why blood HAMA should always be checked before administration of a murine mAb. Furthermore, the following reaction, previously referred to as serum sickness, displays typical symptoms of allergy which may be harmful for the patient. Thus, treatment with murine antibodies is limited to patients without HAMA, and the potential for repeated treatments is poor. With modern gene technology, however, humanized versions of promising mAbs are now being developed, which are less prone to cause allergic reactions in humans [33]. In fact, the murine mAb used in paper I and III of this thesis, MX35, has just recently been made available in a humanized version, rebmAb200 [34].

1.2.3 Radionuclides

Radionuclides are the effectors of RIT in the meaning that the ionizing radiation emitted upon radioactive decay is cytotoxic. By labeling tumor specific mAbs with radionuclides, delivery of radionuclides to tumor cells can be achieved. As the radionuclides eventually decay, the surrounding tissue will be bombarded with ionizing radiation. Ionization of the DNA

molecule may give rise to damages, e.g., base damages, single strand breaks or double strand breaks. DNA damages are continuously induced by natural causes, including exposure to ionizing radiation from natural sources, but they rarely cause any problems because normal cells have a good capacity for repairing its DNA. If the frequency of damages is increased, however, for instance by deliberate irradiation, the cells may not be able to repair and recover due to the complexity of having many damaged sites simultaneously, and this is what RIT aims at achieving in tumor cells.

A radionuclide is an atom with an unstable nucleus. By radioactive decay, the nucleus transforms to a different atom with lower energy state and in that process energy is released by emission of neutrons, charged particles or photons. The decay products leave the decay site and eventually deposit their excess energy by interactions with the surrounding material. The energy deposition pattern after a radioactive decay is determined by the character, yield and energy of the decay products. In RIT, deposition of energy close to the decay site is desirable for maximum impact on the targeted tissue. This can be achieved with radionuclides which decay by emission of charged particles, in particular beta-, Auger-, and alpha-emitters.

As a charged particle passes through a material it leaves behind a track of ionizations caused by a series of interaction processes. In each interaction a small amount of kinetic energy is transferred from the charged particle to an electron in the surrounding material. If the transferred energy exceeds the electron binding energy, the electron will leave its atomic orbit and a vacancy in the electron shell is created, i.e. an ionization of the atom occurs. Each interaction process causes the charged particle to incrementally slow down. The amount of energy transferred in each interaction process is stochastic, but since a very large number of interactions are required to stop a charged particle, it is possible to predict the expected range or path length for a charged particle depending on its charge, mass and initial kinetic energy. Furthermore, the amount of energy deposited per unit path length in a certain material can be predicted, a radiation quality property defined as the linear energy transfer (LET) with unit $\text{keV } \mu\text{m}^{-1}$. LET is commonly used to classify different types of ionizing radiation depending on the character of the ionization track induced. High-LET radiation ($>10 \text{ keV } \mu\text{m}^{-1}$), e.g., protons, alpha particles, and heavy ions, leave relatively short, straight and dense ionization tracks, while low-LET radiation, e.g., electrons, positrons and photons, leave winding and sparse ionization tracks. For charged particles, LET increases along the ionization track as a consequence of the decreasing kinetic energy of the particle. At the end of the track, right before the particle comes to rest, LET reaches a maximum, the Bragg peak.

Due to the high LET, α -particles are considered to have a higher relative biologic effect (RBE) per unit absorbed dose than radiation qualities of low LET. Acute effects of α -particles, such as therapeutic effect on tumor cells and direct damage to normal tissues has been shown to have an RBE=1-15 [35-38]. The large range shows that RBE may differ depending on the end point, radiation sources and cell types studied [39]. The cell cycle position of the irradiated cells has also been shown to influence the radiation sensitivity, specifically cells in late S-phase and mitosis have a higher radiation sensitivity for both high- and low-LET [40]. This finding indicates that tumor cells may be more sensitive to radiation, since the distribution of cells between different cell cycle positions can be expected to be shifted towards these stages in tumor cell populations compared to normal cell populations. For stochastic effects, the relative effect of α -particles may be even higher. Current recommendations from the International Commission of Radiation Protection (ICRP) suggest that α -particle radiation is 20 times more likely to induce cancer than low-LET radiation [41]. Therefore, the risks associated with α -particles must be carefully considered in the development and implementation of α -RIT.

RIT of ovarian cancer, which was the focus of this thesis, has to date primarily been tried with β -emitting radionuclides, e.g., ^{90}Y ($T_{1/2} = 64.1$ h, $E_{\beta,\text{mean}} = 933$ keV), ^{131}I ($T_{1/2} = 8.02$ d, $E_{\beta,\text{mean}} = 192$ keV), and ^{177}Lu ($T_{1/2} = 6.65$ d, $E_{\beta,\text{mean}} = 149$ keV), with average ranges in soft tissue 4.0, 0.42 and 0.28 mm respectively [42-48]. But, in a randomized phase III study using ^{90}Y -HMFG1 against residual ovarian cancer, results showed little or no efficacy [49]. The range of β -particles is long in relation to the dimensions of a cell; an average ovarian cancer cell is 20-30 μm in diameter. Long range can be advantageous for large tumors, because each β -particle may traverse and irradiate many cells (cross-fire), thus relaxing the requirement of primary targeting of each tumor cell, and thus reducing the effect of inhomogeneous intratumoral distribution. Treatment of microscopic ovarian cancer, i.e., microtumors and single cells, with β -emitters may however be ineffective because a low fraction of absorbed energy in targeted tumor cells and low probability for tumor cure can be expected. For that purpose, an α -emitter may have better potential [50]. The short range (<100 μm) and high energy (3-10 MeV) of α -particles give a high fraction of absorbed energy in targeted tumor cells. Still, the range is long enough to facilitate cross-fire irradiation of adjacent cells. The energy deposition pattern conforms well to the dimensions of microscopic tumor cell clusters. Several groups have shown therapeutic efficacy of α -RIT in preclinical studies [51-53] and recently, Meredith et al. treated three ovarian cancer patients in a phase I trial of IP

^{212}Pb -TCTM-trastuzumab [54] with results similar to ours as presented in paper I and III of this thesis.

The list of potential radionuclides for α -RIT is not long [55, 56]. ^{212}Pb ($T_{1/2} = 10.64$ h) is not an α -emitter in itself, but can be used as an *in vivo* generator of α -particles. ^{212}Pb decays by β -emission to ^{212}Bi ($T_{1/2} = 60$ min) which in turn has a two-branched decay, both resulting in the prompt emission of α -particles with energies 6 and 8.8 MeV respectively. The time-delay from primary decay to emission of α -particles, however, limits the potential uses of ^{212}Pb . Upon the primary decay, the chemical bond between the radionuclide and the carrier molecule is broken and there is obvious risk that the radioactive daughter escapes the targeted tissue before it decays.

^{225}Ac ($T_{1/2} = 10$ d) is similar to ^{212}Pb , in the sense that it generates a series of α -particles in its decay chain, the majority of which are emitted within 5 min of the primary decay. But, α -emitting daughter ^{213}Bi ($T_{1/2} = 45.6$ min) is also part of the decay chain, which causes the same problem as described for ^{212}Pb above. Both ^{212}Pb and ^{225}Ac can be useful for RIT, but the fact that the specific targeting facilitated by the carrier molecule is lost after the first decay may be problematic.

Another use of ^{225}Ac is as parent nuclide in an $^{225}\text{Ac}/^{213}\text{Bi}$ generator, which can be eluted for ^{213}Bi every few hours [57]. With its short half-life of 45.6 min, ^{213}Bi is best suited for malignancies which are readily accessible for targeting and so far ^{213}Bi has been used for treatment of leukemia and intracavitary treatment of glioma in humans [58-60]. Preclinical investigations for many other applications of ^{213}Bi , including pretargeted RIT, are ongoing [61-65].

Furthermore, ^{227}Th ($T_{1/2} = 11.4$ d) has been proposed for treatment of breast cancer [66, 67], ovarian cancer [20] and bone metastasis [68]. And, although not labeled to antibodies, bone-seeking α -emitter ^{223}Ra ($T_{1/2} = 11.4$ d) have been tried for treatment of bone metastasis with good results. $^{223}\text{RaCl}$ was the first α -radiopharmaceutical to be approved by the FDA in 2013 for treatment of bone metastasis in castration-resistant prostate cancer patients and is now commercially available under trade name Xofigo®, Algeta ASA, Bayer [69].

^{211}At ($T_{1/2} = 7.21$ h) is considered an interesting α -emitter for RIT thanks to its medium ranged half-life and the lack of long-lived alpha emitting daughters. The development of ^{211}At -RIT is however progressing slowly, in part because of limited availability to ^{211}At . Nevertheless, two clinical studies with ^{211}At have been reported. Zalutsky et al. treated a group of patients suffering from

recurrent glioma with ^{211}At -81C6 in a surgically created resection cavity [70]. The second was the trial of IP ^{211}At -RIT for ovarian cancer reported on in Papers I and III of this thesis. Needless to say, both clinical studies were preceded by extensive preclinical investigations [36-38, 52, 71-80].

1.3 The therapeutic window

The concept of the therapeutic window is a way to describe if a therapy is feasible or not. It can be used in many contexts. The therapeutic window is defined as the range of dosages of some therapeutic agent which give the intended effect on a disease while at the same time intolerable negative effects are avoided. In RIT the “dosage” relates primarily to the amount of administered radioactivity, and the “effects” relate to the biologic effects associated with the absorbed doses delivered to tumor tissue and normal tissues respectively. The width of the therapeutic window says something of which patients are eligible for treatment and the margins for dosage. If the range is wide, therapy can be given to all patients who may benefit. If, on the other hand, the window is narrow, therapy should only be given to patients in dire need after careful consideration of alternatives. It should be noted that the therapeutic window only relates to therapeutic efficacy and the risk for complications. Obviously many other factors, e.g., cost, availability, common practice, and (in my dreams) environmental impact, influence the choice of therapy for a given condition.

The tolerability and efficacy of new therapeutic agents are investigated in clinical trials, normally conducted in four phases. Phase I studies are often designed as dose-escalation studies, with the aim to determine tolerability and to identify potential side-effects. In phase II and III, effectiveness within the safety range is investigated on large groups of patients. Monitoring of side-effects and further evaluation of tolerability is included. Comparison of the new therapy with other treatments can be part of the study design in phase III. In order to complete phase II/III studies within reasonable time, they are often conducted as multicenter studies. Phase IV studies are conducted in the general population after clinical approval of the new therapeutic agent to collect information of adverse effects associated with widespread use.

In the development of new therapeutic regimens, it is not uncommon to find that a proposed therapy lacks a therapeutic window, i.e., that therapeutic effect cannot be achieved without severe toxicity, or that the expected therapeutic effect fails. In such case, the clinical trial should be discontinued or, if hope remains, adjustments to the protocol to improve the outcome could

be made. Some factors influencing the width of the therapeutic window in RIT will be discussed in the following text.

Fast and specific delivery of radionuclides to the target tissue is key to achieve a good ratio between tumor and normal tissue irradiation. Choosing the best suited administration route should thus be the first step in an optimization strategy. It should not only facilitate optimal use of the radionuclide, but also minimize irradiation of normal tissues, thus widening the therapeutic window. For therapy of intraperitoneal disease, as was the focus of this thesis, a peritoneal catheter allows direct access to the tumor cells. This gives a high probability for effective targeting of locally confined tumor cells. Irradiation of normal tissues can at the same time be held at a low level, because retention of radioimmunoconjugate to the peritoneal cavity delays escape into the circulation; meaning that some decay will occur before normal tissues outside of the peritoneal cavity are exposed to the radioimmunoconjugate. For short-lived radionuclides, this sparing effect is significant, which was shown by us in Paper I and by Meredith et.al. [54]. Indeed, similar conditions apply to other intracavitary treatments, where direct infusion of the radioimmunoconjugate into the cavity is possible and high retention of the radiopharmaceutical can be expected [70].

To achieve a good therapeutic effect, the absorbed dose deposited in the nuclei of tumor cells must be high enough to induce lethal damage. When the aim is to knock out micro-tumors and single tumor cells, it is imperative that all cells are loaded with a sufficient amount of radiolabeled mAbs, since a low contribution from cross-irradiation can be expected. A fraction of the mAbs administered will be cold, i.e., not radiolabeled, upon reaching the target, either because they were cold from the beginning or because the carried radionuclides are lost to decay. The specific activity is a measure of the amount of radioactivity carried per microgram of mAb at a certain time point. It can be converted to a ratio between radiolabeled and cold mAbs if the molecular mass of the mAb and the physical half-life of the radionuclide are known. If the specific activity is low, there is risk that the binding capacity of individual cancer cells is saturated by cold mAbs which do not contribute to the therapeutic effect. The specific activity may thus influence the absorbed dose to tumor tissue achievable. Preclinical studies indicate that a threshold value for the specific activity may be determined, below which the therapeutic effect is impaired [81, 82]. Indeed, the level of this threshold is dependent on the number of antigenic sites per cell and should thus be evaluated for each system tried. In a nude mouse model of the therapy tried in Paper I and III, that threshold was found to be between 4-16 kBq/ μ g [82]. The stability of the radioimmunoconjugate is also a factor in this context.

Premature detachment of the radionuclide from the mAb leads to a reduction in the specific activity, with possible consequences as described above. However, a more disturbing consequence is that the resulting free radionuclide will be redistributed in the body depending on its biochemical properties. Free radionuclide may also come from incomplete purification of the radioimmunoconjugate after radiolabeling. Naturally, presence of free radionuclides in RIT should be avoided as far as possible, as it contributes primarily to undesired irradiation of normal tissues. This places high demands on the quality and purity of the radioimmunoconjugate. Specific activity, radiochemical purity and stability should all be high in order to deliver an optimized therapy.

To further enhance the therapeutic effect, different types of radiosensitizers have been tried. For instance, treatment with paclitaxel and doxorubicin has been shown to increase the radiation sensitivity by inducing cell cycle arrest in the G2-M phase in multiple myeloma cell lines [83]. The syngenic effect of paclitaxel and ^{213}Bi -RIT has also been shown in a mouse model of intraperitoneal ovarian cancer [84]. In another study, gemcitabine was shown to increase efficacy of ^{212}Pb -RIT of intraperitoneal colon cancer [85]. Furthermore, histone deacetylase inhibitors have been investigated for their ability to radiosensitize cancer cells [86].

The amount of activity given to a RIT patient is in most situations limited by the tolerance of critical normal tissues, e.g., the red bone marrow, kidneys or intestines. The fraction of radiolabeled mAbs which do not bind to the target tissue, and any free radionuclide will be distributed in the body and irradiate the normal tissues. Addition of a clearing agent is one way to increase the excretion rate of unbound mAbs [87]. Another alternative is to block the uptake of mAbs and/or free radionuclide in normal tissues. Larsen et al. investigated seven compounds for this purpose and found that thiocyanite, perchlorate and iodide ions had a blocking effect on uptake of ^{211}At in the thyroid and in the gastrointestinal tract [77]. Thiocyanite and cysteine also significantly reduced uptake of ^{211}At in the lungs and spleen.

1.4 Ovarian Cancer

Ovarian cancer is a family name for cancers originating from cells of the ovaries. The most common form springs from the epithelial cells lining the ovaries, epithelial ovarian cancer, which in turn be differentiated into (among others) serous, mucinous, clear cell and endometrioid epithelial ovarian cancer. Early symptoms include bloating, pelvic pain, urinary issues and difficulty to eat [88]. A correct diagnose may be difficult to discern at an

early stage, because symptoms are vague and common to several other illnesses. Therefore, ovarian cancer is often diagnosed at an advanced stage, when the disease has spread from the ovaries out into the peritoneal cavity. Predominant growth is found on surfaces lining the peritoneal cavity, the peritoneum. Formation of ascites fluid is common.

The majority of patients diagnosed with ovarian cancer are over 60 years of age, see Figure 1. The risk for developing the disease increases strongly with age. Persons with a family history of ovarian, breast or colon cancer have increased risk. In particular, the genes BRCA 1 and 2 are correlated with a high risk [89]. Childbearing, on the other hand seems to have a protective effect [90].

Standard treatment for ovarian cancer includes surgery and chemotherapy. The extent of the surgery depends on the stage of the disease, but it often includes removal of the uterus, ovaries, fallopian tubes and the omentum. The entire abdomen is thoroughly examined for malignant growth and all nodules are excised (optimal debulking surgery), which has been shown to prolong the life of patients [91]. Chemotherapy, e.g., carboplatin or paclitaxel, is given intravenously and sometimes intraperitoneally.

The response to primary treatment is generally good. The majority of seemingly cured patients however recur and approximately 70% of all ovarian cancer patients die of the disease eventually. In Sweden, ovarian cancer was the cause of death for in the mean 620 women per year from 1991-2007 [92]. Hence, new regimens to reduce the recurrence rate of ovarian cancer are much needed. The primary site for recurrence is inside the peritoneal cavity and microscopic remaining disease is thought to be the cause. Boosting adjuvant therapy with IP α -RIT could help eradicating microtumors and single tumor cells confined to the peritoneal cavity. The work presented in this thesis is aimed at developing such therapy.

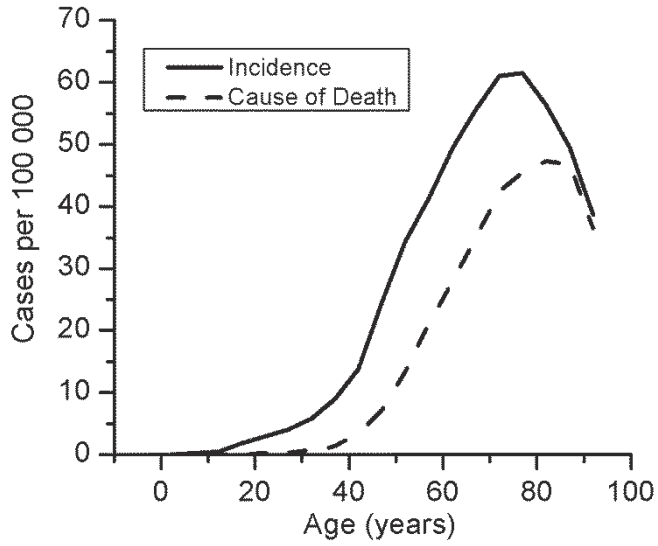


Figure 1 Ovarian cancer incidence and cause of death in Europe and America per 100 000 females. (Data from ICRP 103)

2 AIM

The overall aim of the work presented in this thesis was to develop safe and effective α -radioimmunotherapy for microscopic remaining disease after primary treatment of cancer to improve long term cure rates. Specifically, the alpha-emitter ^{211}At labeled to the monoclonal antibody MX35 targeting ovarian cancer cells was investigated for this purpose. The specific aims of papers I-III of this thesis were

- To investigate the pharmacokinetics of ^{211}At -labeled $\text{F}(\text{ab}')_2$ fragments of mAb MX35 in ovarian cancer patients when infused intraperitoneally with a large volume of icodextrin.
- To estimate absorbed doses to tissues and organs for individual patients undergoing IP ^{211}At -RIT.
- To identify organs or tissues at risk for deterministic effects as a consequence of IP ^{211}At -RIT.
- To investigate the radiation tolerance of one such tissue, namely the peritoneum.
- To estimate absorbed doses to tissues and organs for a general patient undergoing IP ^{211}At -RIT.
- To estimate the effective dose associated with IP ^{211}At -RIT.

3 PATIENTS AND METHODS

3.1 Clinical study

3.1.1 Patients

Paper I included clinical data from nine patients participating in a phase I study of IP $^{211}\text{At-MX35 F(ab')}_2$ for minimal residual ovarian cancer in the peritoneal cavity. In paper III complementary data from another three patients (No. 10-12) enrolled in an expansion of the same clinical study was included. Eligible patients were in remission from recurrent ovarian cancer determined by cancer antigen 125 (CA-125) blood concentration and laparoscopic examination of the peritoneal cavity. Normal hematology, liver function, creatinine levels, and HAMA were required. Patients were enrolled after providing informed consent to the study protocol which was approved by the Regional Ethical Review Board in Göteborg and by the Swedish Medical Products Agency. All patients had undergone surgery following first and second line chemotherapy, taxol and paraplatin being the most prevalently used drugs. Patients No. 3 and 5 had also undergone external radiation therapy directed towards the pelvic region. The patients were 36-69 years of age (median: 52 y) at the time of $^{211}\text{At-RIT}$.

3.1.2 Clinical protocol

A Tenckhoff peritoneal catheter, Tyco Healthcare, was implanted in conjunction with the laparoscopic examination performed to exclude presence of macroscopic intraperitoneal ovarian cancer. A peritoneal scintigraphy was made using $^{99\text{m}}\text{Tc-LyoMMA}$ in peritoneal dialysis fluid icodextrin, Extraneal[®], Baxter, to ensure access to the entire peritoneal cavity via the catheter. The therapy comprised an IP 24h-dwell of $^{211}\text{At-MX35 F(ab')}_2$ in 1-2 L icodextrin. The administered activity, or rather activity concentration, was escalated from 34 – 355 MBq (20 – 215 MBq/L). For patients No. 1-9, the infusion included a trace amount of ^{125}I -human serum albumin ($^{125}\text{I-HSA}$). Samples of peritoneal fluid and blood were collected at regular intervals during the 24h-dwell. Blood sampling was continued until 48h. All urine was collected from the start of the therapy until the patient was released from the hospital after 48h. 2-5 whole-body scintigraphies and 0-2 single photon emission computed tomographies (SPECTs) were acquired with a gamma camera to monitor the in vivo activity distribution.

Small adjustments to the protocol were made during the course of the study as a consequence of preliminary results. Starting with patient No. 6, KClO_4 (or KI, Pat. No. 9) was administered twice prior to therapy to prevent accumulation of ^{211}At in the thyroid. Also starting with patient No. 6, a trace amount of $^{51}\text{Cr-EDTA}$ was added to the IP infusion in an attempt to estimate the area of the peritoneal membrane exposed to the therapeutic fluid (not analyzed). The addition of a third radionuclide however made analysis of collected samples complex, why use of $^{51}\text{Cr-EDTA}$ was discontinued after patient No. 8. From patient No. 7, SPECT imaging was complemented with computed tomography (CT) imaging.

3.2 Animal study

3.2.1 Animals

Results from animal experiments were reported in Paper II. Female BALB/C nu/nu mice were used. The mice were kept under standardized conditions, as stipulated by the Swedish animal welfare agency, at the laboratory for experimental biomedicine, University of Gothenburg, Sweden. They were housed in groups of ten in dedicated cages with access to food and water ad libitum. Their weight and appearance was monitored regularly. Approval from the Ethics Committee for Animal Research at the University of Gothenburg was obtained for all experiments.

3.2.2 Short term experiments

Short term experiments were performed in preparation of the long term experiment described in the following section. Their purpose of these experiments were to i) estimate the IP fluid activity concentration after injection of $^{211}\text{At-trastuzumab}$; to be used for calculating the absorbed dose to the peritoneum, ii) estimate the rate of absorption of an IP injection in mice; also for peritoneum dosimetry, and iii) develop a method for measuring the peritoneal clearance rate of a small inert tracer.

Ten mice were injected IP with $^{211}\text{At-trastuzumab}$ and sacrificed at 60 (n=5) or 200 (n=5) min. Samples of IP fluid and blood were collected and analyzed for activity concentration. An increase in the IP fluid concentration was observed, $131\pm 11\%$ at 200 min, which may be explained by resorption of water from the IP fluid. Activity was also found to increase in plasma.

The volume of remaining fluid after IP injection was investigated by a direct volume recovery method. Animals in groups of 4-9 were sacrificed at

different points in time after IP injection. The abdomen was opened and wiped dry with pre-weighed pieces of gauze. By weighing the soaked pieces of gauze again the amount of IP fluid collected could be determined. The results indicated an initial fast absorption of fluid of approximately 10% of the infused volume, which was 700-800 μL , following an absorption rate of $2.6 \pm 0.4 \mu\text{l min}^{-1}$.

We were interested in finding a way to estimate the rate constant for diffusion across the peritoneal membrane, k_1 , which we hypothesized could be an indicator of the status of the peritoneum after irradiation. The method for evaluation was to be minimally invasive so that repeated measurements could be made without compromising the welfare of the animals. The *in vivo* kinetics of $^{99\text{m}}\text{Tc-DTPA}$ and $^{51}\text{Cr-EDTA}$ were investigated for this purpose. The tracers were injected intravenously or intraperitoneally following evaluation of plasma and IP fluid concentrations in a series of small experiments. Similar renal filtration rates were found for the two tracers, indicating that one could be interchanged for the other in that respect. Furthermore, the results were used to create a simple compartment model for the kinetics involved, see Figure 2.

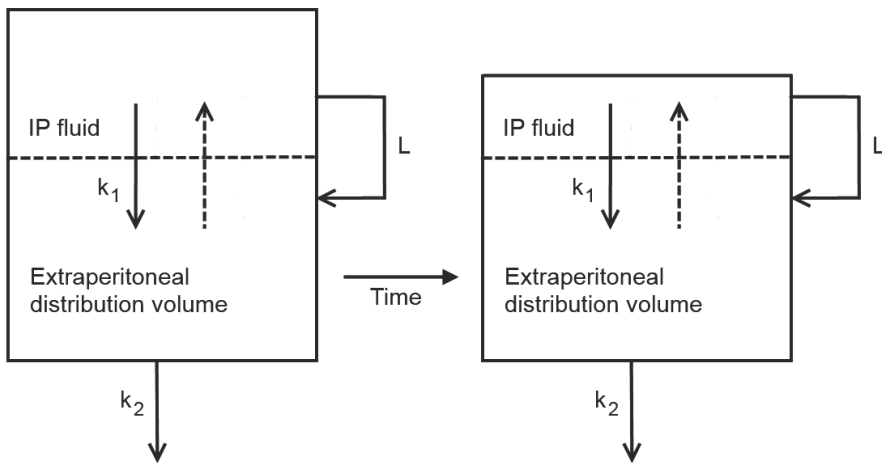


Figure 2 A compartment model for the transport of an intraperitoneally injected tracer. The upper and lower compartments, separated by the peritoneal membrane, represent IP fluid and the extraperitoneal distribution volume respectively. Transport routes for tracer are indicated by arrows: k_1 = rate constant for diffusion across the peritoneal membrane, k_2 = rate constant for renal filtration and L = lymphatic drainage of the peritoneal cavity.

An equation describing the plasma (extraperitoneal) concentration, c_{ep} , of an IP injected tracer as a function of time was derived from the compartment model. We found that by fitting experimental plasma concentration data to this equation, k_1 could be estimated if all other parameters were known.

$$\frac{dc_{ep}}{dt} + k_2 c_{ep} = \frac{c_{ip}(0)}{V_{ep}} e^{-k_1 t} [L + k_1 (V_{ip}(0) - Lt)]$$

L was assumed not to vary between animals and was set to $2.6 \mu\text{l min}^{-1}$ as determined in a previous experiment. The renal filtration rate constant, k_2 , has been shown to be dependent on the absorbed dose to the kidneys and the time after exposure [74]. Since some irradiation of the kidneys was expected in the planned long term experiment, see section 3.2.3, where peritoneal clearance measurements were to be part of the follow up, evaluation of k_2 had to be performed each time k_1 was to be evaluated. The plasma activity concentration of IP injected $^{99\text{m}}\text{Tc-DTPA}$ in three consecutive samples was used for this purpose; the technique was described in detail previously by Bäck et al. [74]. The extraperitoneal distribution volume, V_{ep} was also evaluated in this procedure. The values of k_2 and V_{ep} obtained were used as constants in the above equation in the next step, where the plasma activity concentration of IP injected $^{51}\text{Cr-EDTA}$ in three consecutive samples was fitted with k_1 as the only unknown variable; $c_{ip}(0)$ and $V_{ip}(0)$ being the activity concentration and injection volume of the IP injection respectively. Finally, the peritoneal clearance rate was determined with the equation

$$Cl_{P \rightarrow Pl} = 100 \frac{k_1}{c_{ip}(0)}$$

To minimize the suffering for the animals exposed to the experiment, IP and IV injections were made (more or less) simultaneously and the following three blood samples were analyzed for both tracers. IV injections and blood samplings were done via the tail vein after preheating the animal for a few minutes with an IR lamp to stimulate dilation of the tail vein, which reduces the risk of damaging the vein upon puncturing it. Special care was taken to avoid the injection site when drawing blood samples.

3.2.3 Long term experiment

Groups of 6-12, a total of 42, healthy mice were injected intraperitoneally with increasing levels of radioactivity in the form of ^{211}At -labeled trastuzumab with the purpose to irradiate the peritoneum. The biodistribution of IP ^{211}At -trastuzumab was studied previously by Palm et al. [93], revealing high uptake in the thyroid and moderate uptake in lungs, spleen, kidneys, stomach and liver. Furthermore, blood counts nadir has been shown to occur 5 days after injection of ^{211}At -labeled mAb [36]. The treatment was therefore given in 2-4 fractions, 2-3 weeks apart, to achieve high absorbed doses to the peritoneum, while avoiding lethal myelotoxicity by allowing the animals to recover between fractions [94].

The mice were followed for up to 34 weeks after the first ^{211}At -mAb injection. Peritoneal clearance measurements were performed on a few occasions in the range of weeks 14-30. At the end of the study, or earlier for mice in poor health, the mice were sacrificed and dissected. The ventral part of the peritoneum and the mesenteric windows were macroscopically examined and photographed. Biopsies of ventral peritoneum were fixated in Bouin's solution for subsequent immunohistochemical staining against plasminogen activator inhibitor (PAI-1) and against calprotectin. Biopsies for morphological assessment were stained with hematoxylin and eosin (H&E). All sections were compared and evaluated individually by two blinded observers.

3.3 Radionuclides

3.3.1 ^{211}At

Astatine (At) with atomic number 85 is an extremely rare element in nature. It occurs only as part of the decay chain of long-lived heavy radionuclides. Mendeleïev, the father of the periodic table, predicted the existence of element 85 long before it was found. It was given the preliminary name eka-iodine, because of its position below iodine in the halogen group. The element was synthesized for the first time in 1940 [95]. The discoverers, Corson, MacKenzie and Segré, realized that all isotopes of element 85 are radioactive and changed the name to astatine after the greek word αστατοζ (unstable). Being a halogen, At readily forms negative astatide ions. Its chemical oxidation states have however been shown to include I, III, V and VII, indicating that At also have metallic properties [96].

Of all astatine isotopes, ^{211}At ($T_{1/2} = 7.214\text{ h}$) is the only obvious candidate for therapeutic use. That is because its decay is associated with rapid emission of α -particles. ^{211}At decays either by electron capture to ^{211}Po ($T_{1/2} = 0.512\text{ s}$) or by α -particle emission to ^{207}Bi ($T_{1/2} = 32.9\text{ y}$). Both daughters decay to ^{207}Pb by α -particle emission and electron capture respectively.

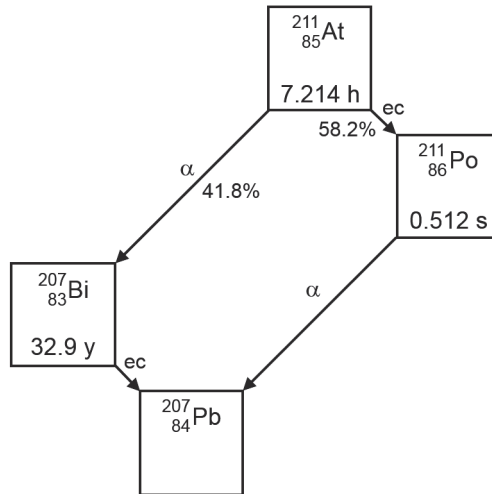


FIGURE 3 The branched decay chain of ^{211}At .

The ^{211}At decay chain is primarily associated with the emission of α -particles with energies 5.867 MeV (^{211}At origin) and 7.450 MeV (^{211}Po origin). The ranges in water for the α -particles are 48 and 70 μm and the mean LET is 122 and 106 keV/ μm respectively. Towards the end of the α -particle track, the LET increases to $\sim 230\text{ keV}/\mu\text{m}$ [97]. However, a spectrum of characteristic x-rays and a few gammas are also emitted, see Figure 4, which makes radioactivity determination with a standard dose calibrator and imaging with a gamma camera possible.

^{211}At is produced by irradiating a ^{209}Bi target with He^{2+} ions via the $^{209}\text{Bi}(\alpha, 2n)^{211}\text{At}$ reaction. The reaction can be carried out utilizing a cyclotron with capacity to accelerate helium ions [98]. The energy of the He^{2+} ions should be above 29.1 MeV to avoid simultaneous production of ^{210}At ($T_{1/2} = 8.1\text{ h}$) [99], which decays to the α -emitter ^{210}Po ($T_{1/2} = 138\text{ d}$) and is difficult to separate from ^{211}At .

The ^{211}At used in this thesis was produced at the PET and Cyclotron Unit, Rigshospitalet, Copenhagen, Denmark. Irradiated ^{209}Bi targets were transported by car to Gothenburg. The $^{209}\text{Bi}/^{211}\text{At}$ layer on the target surface was mechanically shaved off using a custom made tool and collected in a quartz glass tube. A dry-distillation technique was then used to separate the ^{211}At from the target shavings [100]. The tube with shavings was placed in a tube furnace at $670\text{ }^\circ\text{C}$, following prompt evacuation through a PEEK capillary placed in a cooling bath of dry ice and ethanol ($-78\text{ }^\circ\text{C}$) where the ^{211}At was trapped. The ^{211}At was then eluted from the PEEK capillary with a small volume of chloroform, transferred to a reaction vial for further workup after full evaporation of the chloroform.

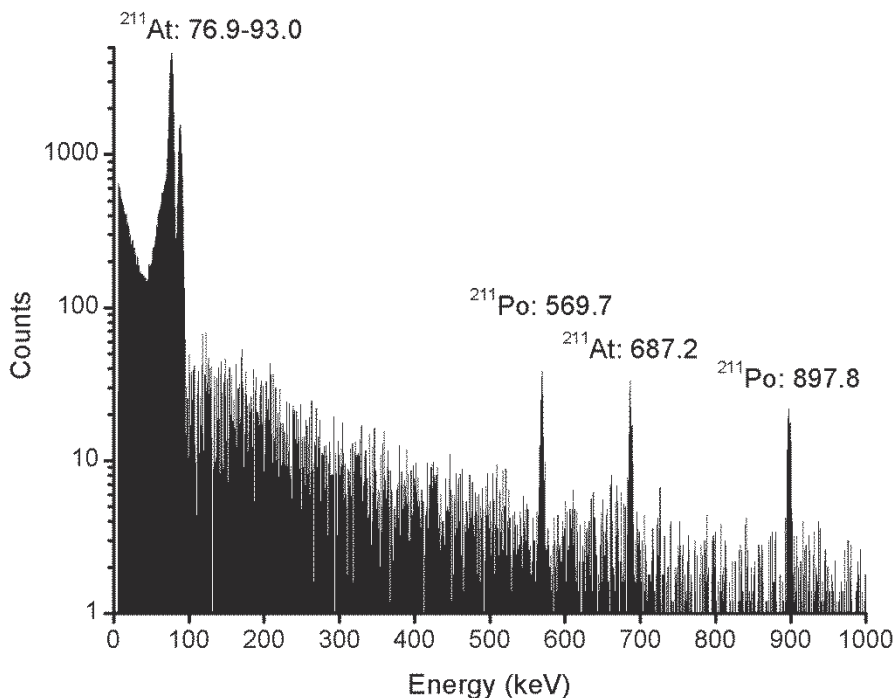


Figure 4 The photon spectrum of ^{211}At , including emissions from short-lived daughter ^{211}Po , acquired with a high-purity germanium detector.

3.3.2 ^{125}I

The iodine isotope ^{125}I ($T_{1/2} = 59$ d) is produced in a nuclear reactor and is used for various biologic assays, as a tracer in nuclear medicine when a long half-life is needed, and sometimes in brachytherapy. Its decay is associated with emission of low energy photons (<35 keV) and Auger electrons. ^{125}I is commercially available and was purchased labeled to human serum albumin, ^{125}I -HSA.

3.3.3 ^{51}Cr

^{51}Cr ($T_{1/2} = 27.7$ d) emits gamma rays at 320 keV and is commercially available as a dissolved salt or chelated to EDTA. The ^{51}Cr -EDTA used in Paper II was purchased from GE Healthcare.

3.3.4 $^{99\text{m}}\text{Tc}$

$^{99\text{m}}\text{Tc}$ ($T_{1/2} = 6.0$ h) is the most commonly used radionuclide in nuclear medicine. Its 140 keV gamma emission is utilized for gamma camera examinations of various conditions including heart, lung, breast, thyroid, kidneys, skeleton and tumors. $^{99\text{m}}\text{Tc}$ is conveniently eluted from a generator holding the parent nuclide ^{99}Mo ($T_{1/2} = 65.94$ h) in the form of pertechnetate ions ($^{99\text{m}}\text{TcO}_4^-$). A number of kits are available for preparation of different $^{99\text{m}}\text{Tc}$ -pharmaceuticals. $^{99\text{m}}\text{Tc}$ chelated to DTPA was used in Paper II, and in Papers I and III, $^{99\text{m}}\text{Tc}$ was labeled to LyoMMA. Both radiopharmaceuticals were prepared using kits from Mallinkrodt Medical.

3.4 Monoclonal antibodies

3.4.1 MX35

The monoclonal antibody MX35 was developed by immunization of mice with ovarian carcinoma specimens [101]. A hybridoma cell line has been established for its production [102]. The antibody recognizes the 95 kDa plasma membrane sodium-dependent phosphate transporter protein 2b (NaPi2b) [19]. High expression of NaPi2b has been found on the cell membrane of serous epithelial cancer samples, the histological subtype which stands for the bulk of malignant tumors of ovarian origin [17, 18]. The median level of NaPi2b-expressing cells was 90%, range 0-100% between samples. Expression of NaPi2b has also been shown in lung, kidney, testis, liver, mammary gland and salivary gland tissues [103-107]. Clinical grade MX23 F(ab')₂ fragments, 110 kDa, (Strategic Biosolutions, Newark, USA) provided by the Memorial Sloan Kettering Cancer Center, New York, USA, were used in the phase I study reported in Papers I and III. A humanized version of MX35 has recently been made available, RebmAb200 [34]. The possibility for using RebmAb200 instead of MX35 in future clinical studies on IP ²¹¹At-RIT is currently under investigation.

3.4.2 Trastuzumab

The trastuzumab antibody is an FDA approved therapeutic drug recognizing the 185 kDa human epidermal growth factor receptor type 2 (HER2). Its main use is in adjuvant treatment of metastatic breast cancer [108, 109]. It has also been utilized as targeting vector in preclinical radioimmunotherapy of HER2-positive tumors of other origins [93, 110-113]. ²¹¹At-labeled trastuzumab (Herceptin, Roche) was used in Paper II for irradiation of the peritoneum in tumor free mice.

3.5 Radiolabeling with ^{211}At

The method for astatination of mAbs, or fragments thereof, was improved during the course of the work with this thesis. The first nine patients participating in the phase I clinical study reported on in Paper I were treated with a radiopharmaceutical prepared in a two-step process with yields around 20-30% [114]. The ^{211}At was first labeled to an intermediate, m-MeATE, using *N*-iodosuccinimide (NIS) as an oxidizing agent, following conjugation to an antibody with a 30 min incubation time.

All ^{211}At -labelings for the studies reported on in Paper II and III were instead prepared with a one-step procedure [115]. Here, conjugation of m-MeATE and antibody was prepared in advance. 25 $\mu\text{mol/ml}$ m-MeATE in dimethyl sulfoxide and 3 mg/ml mAb in 0.2 M sodium carbonate buffer, pH 8.5, in 5- to 10-fold molar excess, was incubated for 30 min, after which the immunoconjugate fraction was isolated on a NAP-5 column eluted with 0.2 M sodium acetate buffer, pH 5.5. The astatination procedure started with activation of a dry residue of ^{211}At with 20 μl 133 μM NIS in MeOH:1% HAc immediately prior to adding 300 μl 2 mg/ml m-MeATE-mAb to the reaction vial. After 1 min incubation, 3 μl 18 mM NIS was added, following another 1 min incubation. The reaction was stopped by addition of 5 μl 50 mg/ml L-ascorbate. The radioimmunoconjugate was isolated on a PD-10 column eluted with 9 mg/ml sodium chloride solution. Radiochemical yields were around 80% with this method.

Samples of the radioimmunoconjugate were analyzed prior to administration to patients or animals. The radiochemical purity was evaluated by fast-protein liquid chromatography (Äkta Purifyer 10, GE Healthcare) and by methanol precipitation; >90% was required for administration to patients. The Lindmo assay [116] was used to determine the immunoreactive fraction (IRF), i.e., the fraction of mAbs which binds to antigen-expressing cells [117]. Specifically, MX35 labelings were evaluated with NIH:OVCA-3 cells [118] requiring IRF >40% after 45 min incubation for approval. Trastuzumab labelings were not tested for IRF, because ^{211}At -labeled trastuzumab was only used for unspecific irradiation in non-tumor bearing animals.

Preparation of radiopharmaceuticals intended for administration to patients were performed under sterile conditions in clinically approved facilities at the Nuclear Medicine Department, Sahlgrenska University Hospital, Göteborg, Sweden.

3.6 Radioactivity measurements

A well ionization chamber (CRC-15 dose calibrator, Capintec) was used to measure activity $>1\text{MBq}$. Samples of low activity, $<10\text{ kBq}$, were measured in a NaI(Tl) gamma counter (Wizard 1480;Wallac). Samples containing two different radionuclides, e.g., $^{211}\text{At}/^{125}\text{I}$ or $^{99\text{m}}\text{Tc}/^{51}\text{Cr}$, were measured twice with dual energy discrimination windows; the second time after virtually complete decay of the radionuclide with shorter half-life. This procedure allowed correction for spillover counts between energy discrimination windows. The well ionization chamber and the gamma counter were cross-calibrated at regular intervals for the radionuclides concerned.

3.7 Gamma camera imaging

Imaging of ^{211}At with a gamma camera in patients and phantoms is possible utilizing the characteristic x-rays emitted by ^{211}At upon decay [119]. The largest contributions to the spectrum have energies 77 keV (11.7 %), 79.6 keV (19.4%), 89.6 keV (2.2%) and 90.1 keV (4.2%) [120]. In Papers I and III a dual-headed gamma camera (Millenium VG; GE Healthcare) with a medium energy collimator was used for planar and single photon emission computed tomography (SPECT) ^{211}At -imaging. The energy discrimination window was fixed at $79 \pm 15\%$ keV. The gamma camera sensitivity for ^{211}At with these settings was estimated to 3.9×10^{-5} cps/Bq by static imaging of a small Petri dish containing ^{211}At .

Whole body scans of patients were made in conjugate view with a scan speed of 10 cm/min. A neck phantom was used to estimate the sensitivity for ^{211}At uptake in the thyroid in anterior whole body scans to 7.65 counts/kBq.

SPECT scans covering the area from the pelvis to the heart were acquired in 60 or 120 projections, 20 or 30 s per frame. SPECT scans were combined with low dose computed tomography acquired with a Hawkeye system connected to the gamma camera (SPECT/CT) for selected patients.

Reconstruction of SPECT images was made using an ordered subsets expectation maximization (OSEM) algorithm implemented in *in house* software. CT image based attenuation correction with linear attenuation coefficient 0.18 cm^{-1} was incorporated in the reconstruction process. SPECT projections were smoothed with a Gaussian filter and corrected for scatter prior to reconstruction. Scatter correction was done by convolving the projection images with a filter matrix with the value $1-A$ in the central position and $-A \exp(-Br)$ in all other positions [121], r = distance to the

central position in pixels. The filter parameters A and B describe the amplitude and slope of an idealized distribution of scattered photons surrounding a point source respectively. Radial symmetry and exponential decline were assumed. Several factors, e.g., the photon energy used for imaging, the dimensions of the imaged object and the source depth, influence the shape of the scattered photon distribution [122]. The filter parameters used for scatter correction of ^{211}At projection images were $A = 0.0027$ and $B = 0.15 \text{ pixel}^{-1}$; the pixel size was $4.42 \times 4.42 \text{ mm}^2$. Scatter correction with these parameters reduced the total number of counts in reconstructed images by approximately 40%.

4 RADIATION DOSIMETRY

Radiation dosimetry is concerned with measuring and calculating the absorbed dose. The standard international (SI) unit for the absorbed dose is Gray (Gy), defined as the mean energy imparted (J) per unit mass (kg) of a specified material as a consequence of interaction processes with ionizing radiation. The absorbed dose is important because it is predictive of the biologic response of tissues, organs or organisms exposed to ionizing radiation. In the field of medical physics, radiation dosimetry is the main tool for dose planning of radiation therapy, for risk assessment and optimization of therapeutic and diagnostic procedures and for radiation protection of personnel.

Formalisms for internal radiation dosimetry, i.e. schemas for calculations of the absorbed dose from radioactive sources within the body, have been stipulated by the International Commission for Radiological Protection (ICRP) and the Committee on Medical Internal Radiation Dose (MIRD) of the Society of Nuclear Medicine and Medical Imaging, USA. In a recent publication from MIRD, the convergence of the two formalisms to a common standard is attempted, including quantities relevant for long term risk estimations, e.g., equivalent dose and effective dose, originally defined by the ICRP [123]. In principle, the body is divided into a number of source and target volumes. Source volumes, r_S , contain a radioactive substance of some sort over some period of time. Target volumes, r_T , are tissues to which the absorbed dose is to be calculated. Source and target volumes are independent entities that can be defined on any scale from whole organs down to sub-cellular structures. However, a certain degree of homogeneity should apply regarding the radioactivity distribution within source regions and the tissue composition within target regions. According to the MIRD formalism, the dose rate in a target tissue, $\dot{D}(r_T, t)$, is the sum of contributions to the absorbed dose rate in the target from all source regions, as summarized by the equation

$$\dot{D}(r_T, t) = \sum_{r_S} A(r_S, t) S(r_T \leftarrow r_S, t)$$

where A is the time-dependent activity (Bq) of a radionuclide in r_S , and S is a quantity describing the mean absorbed dose rate in r_T per unit activity in r_S (Gy Bq⁻¹). Integration of the above equation with respect to time yields the

mean absorbed dose in the target tissue $D(r_T)$. This requires knowledge of the activity in relevant source regions and appropriate S-values.

In nuclear medicine, information regarding the activity distribution in a patient is typically acquired from gamma camera imaging, bodily fluid sampling and pharmacokinetic modelling. Indeed, all of these methods were used in this thesis. The value of S depends on many factors, e.g., the radionuclide used, the sex, age, body mass and height of the patient, and ultimately how source and target volumes are defined.

S-values and similar quantities for source and target volumes in computational reference phantoms of different shapes and sizes have been published for many radionuclides [124, 125]. In paper III, two such resources were used to calculate the absorbed dose attributable to photon emissions from ^{211}At to a selection of tissues for a general patient undergoing IP ^{211}At -RIT. First, the absorbed dose from decays occurring inside the peritoneal cavity was calculated with a computational phantom designed to simulate the IP therapy situation [126]. S-values (dose factors) for ^{211}At in this phantom were available for download from the RADAR project homepage [124]. The total amount of activity present in the peritoneal cavity was estimated by multiplying the activity concentration (measured) with an approximation of the IP fluid volume over the 24-h dwell provided by Baxter, manufacturer of the instillation fluid; the volume peaked at 150% of the initial volume at 18h. Integration over 24h gave the time-integrated activity in the peritoneal cavity needed to calculate the absorbed dose in different organs with the S-values provided for the peritoneal cavity phantom. Second, absorbed doses (photon contribution only) from ^{211}At in circulation were calculated with another computational phantom representing an adult female, also available via the RADAR project homepage [124]. In this case, S-values for ^{211}At were not provided directly, but could be calculated from tabulated specific absorbed fractions (SAFs) for different photon energies. Detailed decay data on the photon emissions from ^{211}At and ^{211}Po [127] were used to convert SAFs to S-values for subsequent use in absorbed dose calculations. The time-integrated activity, i.e., the number of decays, occurring outside the peritoneal cavity was approximated by taking the difference between the total number of decays expected in the first 24h, based on the amount of administered activity, and the number of decays found to occur within the peritoneal cavity. Obviously, these calculations provided only rough estimations. The photon contribution to the total absorbed dose was however $<5\%$ for all organs studied in paper III, why this level of accuracy was considered sufficient.

The energy released in the ^{211}At decay chain is to >99% carried by α -particles with range <100 μm . The short range implies that, when calculating mean absorbed doses, charged particle equilibrium can be assumed even in small volumes, such as a thin layer of fluid in the peritoneal cavity of a mouse or human. Charged particle equilibrium means that net flow of charged particles across the boundary of a subvolume to the whole volume studied is equal to zero. In other words, the energy locally released is equal to the energy locally absorbed; the absorbed fraction $\phi = 1$. This assumption was applied in all calculations of the absorbed dose from α -particles to organs and tissues containing ^{211}At in this thesis, i.e. the equilibrium absorbed dose was calculated. The absorbed dose equation is under such conditions reduced to

$$D(r_T) = \frac{\Delta\phi}{m} \int_0^{T_D} A(r_T, t) dt$$

where Δ = the mean energy released per decay ($\Delta = 1.09 \times 10^{-12} \text{ J Bq}^{-1} \text{ s}^{-1}$ for alpha emissions from ^{211}At and daughter ^{211}Po), m = the mass of target tissue r_T , $A(r_T, t)$ = the activity in r_T as a function of time, and T_D = the dose-integration period. Similarly, absorbed doses to surfaces adjacent to fluids containing ^{211}At , i.e., the peritoneum and the urine bladder epithelium, were calculated as half of the equilibrium dose to the IP fluid and urine respectively.

A more detailed dosimetry was not reasonably achievable with the clinical and preclinical data at hand. It should however be noted that spatial variations in the absorbed dose distribution may be expected on a microscopic scale [128]. Microdosimetric calculations show that an α -particle traversal through a cell nucleus deposits up to 0.3 Gy, which is close to the absorbed dose associated with 37% probability of subsequent cell death [129]. This indicates that a few hits could be sufficient for killing a cell. However, in the scenario of minimal residual disease, millions of tumor cells may be involved, each capable of causing recurrence. In order to have a decent tumor cure probability, all of these cells must be hit by several α -particles. Preliminary results, derived from a subcutaneous tumor model, indicate that the mean absorbed dose to tumors should be at least 10 Gy, corresponding to in the mean 50 hits per cell, for successful therapeutic results [130]. Still, 50 hits is not much compared to how many hits would be required to achieve the same effect with beta-particle irradiation. In fact, the low number of traversals required to kill a cell, is considered the main advantage of using α -

emitters for treatment of minimal disease. Quantification of the uptake of ^{211}At -mAb by *ex vivo* α -camera imaging have shown that high absorbed doses can be achieved locally in successfully targeted microtumors and single tumor cells [131].

Furthermore, the biologic effect per Gy of α -particle irradiation is higher than that of photon or electron irradiation. Differing energy deposition patterns, or LET, is considered to explain the phenomenon. The relative biologic effect (RBE), defined as the ratio between the absorbed doses of low-LET and α -particle irradiation respectively inducing the same biologic effect, is useful for describing or quantifying this difference. Depending on the endpoint used in comparative studies, the value of RBE varies between 1-15 for deterministic effects, e.g., tumor response, cell death or acute detrimental effects on normal tissues [35-37, 39, 40]. For stochastic effects, e.g., cancer induction, an even higher factor, 20, have been suggested by the ICRP under the name radiation weighting factor, w_R [41]. The probability for cancer induction is furthermore different between tissues.

The ICRP have stipulated a system for calculation of the effective dose (E), a quantity for comparison of different irradiation scenarios in relation the risk for cancer induction. Equivalent absorbed doses are first calculated by summing the radiation quality weighted contributions to the absorbed dose for all irradiated tissues respectively. In the next step, equivalent absorbed doses are multiplied by their tissue weighting factors, w_T , respectively, following summation.

$$E = \sum_T w_T \sum_R w_R D_{R,T}$$

The result, E, is an indicator of the long term risk for developing cancer as a consequence of the irradiation. The effective dose was estimated for a general patient undergoing IP ^{211}At -RIT in paper III.

5 RESULTS

5.1 Clinical results

5.1.1 Pharmacokinetics

The pharmacokinetics of intraperitoneally infused ^{211}At labelled to $\text{F}(\text{ab}')_2$ fragmented mAb MX35 was studied in 12 patients. The administered activity was 34-355 MBq mixed in 1-2 L icodextrin solution, resulting in activity concentrations between 20-215 MBq L^{-1} . The radiochemical purity was >92% in all patients and the specific activity was 50-355 MBq mg^{-1} . See Table 1 for the specific amounts administered to each patient.

Table 1 Activity and infusate volumes administered to patients undergoing IP ^{211}At -RIT.

Pat. No.	Administered activity ^{211}At (MBq)	Infusate volume (L)	Initial ^{211}At -concentration (MBq L^{-1})	Specific activity (MBq mg^{-1})
1	34	1.5	22	61
2	48	2.0	24	105
3	40	2.0	20	81
4	42	2.0	21	212
5	92	2.0	46	69
6	103	2.2	47	83
7	119	1.2	101	-
8	83	1.1	73	64
9	65	1.2	53	50
10	297	1.7	180	293
11	333	1.6	203	624
12	355	1.7	215	743

When reporting pharmacokinetic data, physical decay of the radionuclide is often disregarded (decay correction). This is done by applying a radionuclide-specific time-dependent correction factor to measured activity data. Decay corrected data are very useful for analysis of transport of a substance through the body, the pharmacokinetics. When calculating absorbed doses, however, the true activity must be considered. For a radionuclide of short half-life, such as ^{211}At , the difference between decay corrected and non-decay corrected activity data is dramatic. Therefore, both types of data will be accounted for, when appropriate, in the following summary of clinical results.

The infusate fluid used, icodextrin, is an osmotic fluid normally used for peritoneal dialysis. It draws water into the peritoneal cavity, thus causing a volume increase and corresponding concentration decrease of the IP fluid. The volume of the IP fluid was not monitored in the phase I study, but the decay corrected concentration was $45\% \pm 7\%$ (mean ± 1 SD) of the initial concentration (IC) at 24h after instillation, determined by sampling of the IP fluid via the peritoneal catheter. This corresponds to $4.2\% \pm 0.7\%$ IC in true activity concentration. The majority of the administered activity was retained inside the peritoneal cavity for the duration of the 24h-dwell. A small fraction of the activity however gradually appeared in the blood stream. The decay corrected activity concentration in blood increased during the entire studied time span. However, the true activity concentration peaked at around 12 h in blood, see Figure 5 for both IP fluid and blood activity curves.

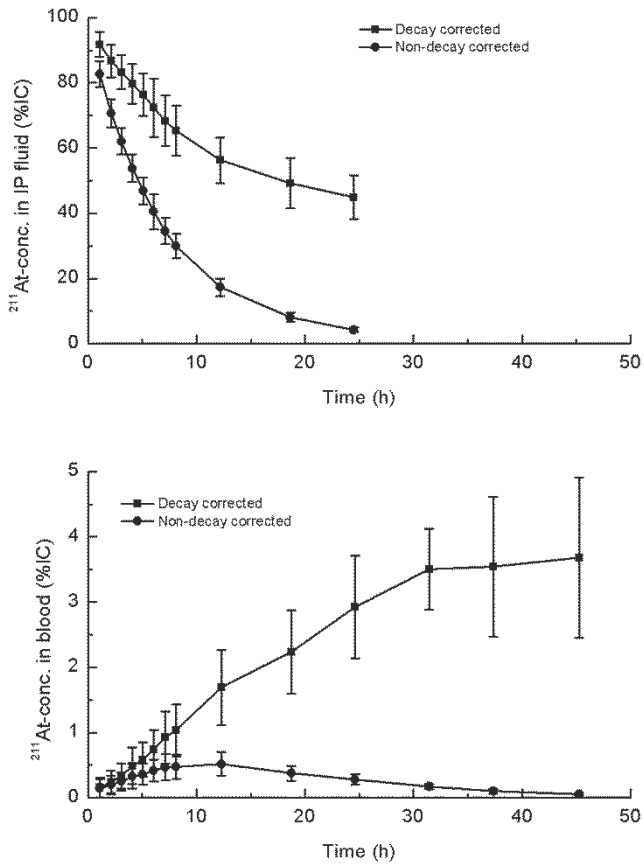


Figure 5 The mean ^{211}At -concentration in IP fluid (upper) and blood (lower) for 12 patients undergoing IP ^{211}At -RIT during $24\text{ h} \pm 1\text{ SD}$. Both IP fluid and blood concentrations are normalized to the initial concentration (IC) of the IP infusate.

Gamma camera images revealed uptake of ^{211}At in the thyroid, which early in the study led to the amendment of a thyroid blocking agent, KClO_4 , to the clinical protocol. The uptake was significantly lower in the following patients. In fact, the thyroid was not possible to distinguish in early (1-5 h) gamma camera scans. However, all patients had apparent ^{211}At uptake in the thyroid at 20 h, see Table 2. A negative correlation between the thyroidal uptake and the radiochemical purity of the infusate was found in patients blocked with KClO_4 , indicating that it is the free ^{211}At that accumulates in the thyroid.

Table 2 The blocking agent used, the radiochemical purity and the thyroidal uptake of ^{211}At at 20h for patients undergoing $\text{IP}^{211}\text{At-RIT}$ in percent of the administered activity (%IA).

Pat. No.	Blocking	Radiochemical purity (%)	Thyroid uptake (decay corrected) at 20 h (%IA)
1	-	93.7	0.63
2	-	96.5	1.89
3	-	95.3	1.50
4	-	97.0	1.58
5	-	98.0	1.06
6	KClO_4	96.7	0.02
7	KClO_4	96.0	0.02
8	KClO_4	96.0	0.09
9	KI	97.5	0.24
10	KClO_4	94.1	0.19
11	KClO_4	96.4	0.03
12	KClO_4	92.3	0.35

The introduction of a blocking agent possibly also affected the rate of urinary excretion. Urine activity data from Patients No. 1, 3, 5, and 9-12 indicate that patients treated with KClO_4 had an increased excretion rate by a factor 2-5, see Figure 6. A possible explanation may be that, the unblocked thyroid acts as a sink, keeping the blood clear of free ^{211}At . When the sink is blocked, the presence of free ^{211}At in blood is increased, following a higher excretion via the kidneys. The amount of activity found in urine, however, exceeds the amount of free ^{211}At present in the infusate from the start. Up to 200% of the initial amount of free ^{211}At was noted at 24h, which suggests that ^{211}At is released from the radioimmunoconjugate during the course of the therapy, or that the radioimmunoconjugate is itself filtered to some extent via the kidneys, or that both of the above apply.

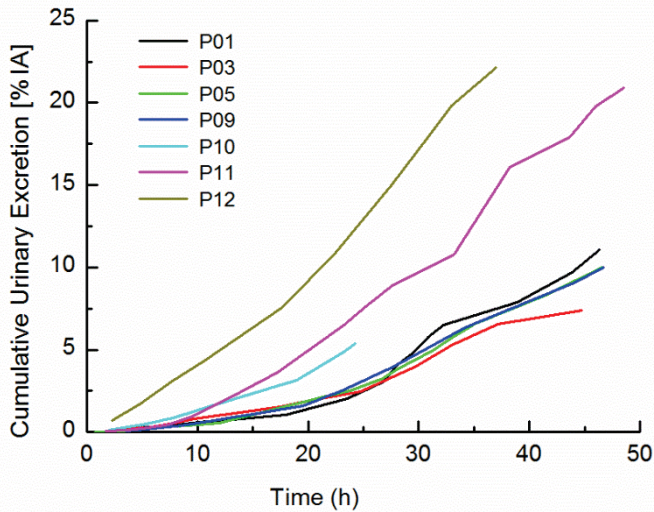


Figure 6 The decay corrected cumulative urine excretion of ^{211}At in selected patients undergoing IP ^{211}At -RIT. Patients No. 10-12 were treated with KClO_4 .

The images and samples collected revealed no accumulation of activity in any organ apart from the thyroid. Nevertheless, uptake of ^{211}At in the liver, lungs, heart, kidneys and breasts was quantified in SPECT images. Quantification was compromised by the large volume of radioactive IP fluid present in the abdomen and by low contrast and resolution due to scatter and a relatively low countrate. SPECT images acquired earlier than 12h were deemed inappropriate for quantitative purposes, at least with the present acquisition protocol which was not optimized for quantitative imaging. A more favorable ratio between tissue and IP fluid activity levels was found at late time points, leading to quantification results less disturbed by scatter. However, only two SPECT-studies acquired at 12h or later were available: one at 12 h from patient No. 11 and one at 20 h from patient No. 12, why the results should be interpreted with some precaution. The uptake levels, expressed as organ-to-blood ratios, were in liver ~ 0.5 , in lungs ~ 1.5 , in heart ~ 0.7 , in kidneys ~ 0.9 , and in breasts ~ 0.2 , based on those two studies.

5.1.2 Dosimetry

Absorbed doses to the peritoneum, the thyroid, the red bone marrow and the urine bladder were calculated for each patient. The results are summarized in Table 3 in plain figures and normalized to the initial concentration of the IP infusate in Figure 7. The normalized data show that the thyroids of unblocked patients were exposed to the highest relative absorbed doses and that treatment with KClO_4 reduced the thyroid absorbed dose per MBq L^{-1} by >90%. Full protection from ^{211}At irradiation was however not achieved. The highest absorbed doses noted in the study, 2-3 Gy, were to the peritoneum of patients exposed to the highest activity concentrations tried.

Table 3 Absorbed doses to selected organs for patients undergoing IP ^{211}At -RIT expressed in mGy.

Pat. No.	Red bone marrow	Thyroid	Peritoneum	Urine bladder
1	3	200	280	13
2	2	590	310	-
3	4	520	290	16
4	3	80	330	-
5	9	820	660	44
6	9	20	690	-
7	9	30	1590	-
8	11	70	910	-
9	6	180	770	30
10	17	490	2300	-
11	29	91	2800	300
12	44	1200	2500	480

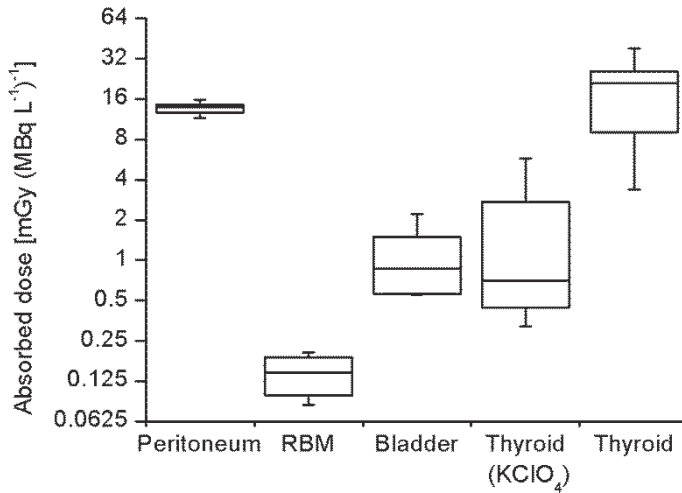


Figure 7 Absorbed doses to selected organs for patients undergoing IP ²¹¹At-RIT, normalized to the initial concentration of the infusate, summarized in box plots showing the maximum, median and minimum values observed. The absorbed dose to the thyroid is presented in two groups depending on treatment with KClO₄.

Absorbed doses to a wider selection of organs and tissues were calculated for a general patient undergoing IP ²¹¹At-RIT with 300 MBq in 1.5 L icodextrin. The aim of these calculations was to find an estimate of the effective dose associated with this type of therapy. Hence, the photon and α -particle contributions to absorbed doses were calculated separately. Computational reference phantoms were used to find the photon contributions. Organ-to-blood ratios, derived from either SPECT quantification or a preclinical biodistribution study [37], in combination with clinical mean blood activity were used to find the α -particle contributions to the organs not accounted for above. The results of these calculations are presented in Table 4. Figures in parenthesis were included for comparison only. The effective dose associated with an IP infusion of 200 MBq ²¹¹At-MX35 F(ab')₂ in 1.5 L icodextrin was <2 Sv. The largest contributors to the effective dose were in descending order the thyroid, the stomach, the lungs and urine bladder.

Table 4 Overview of absorbed dose contributions to the effective dose associated with $IP^{211}At-RIT$.

Tissues	Abs. dose from α -particles [mGy]		Abs. dose from photons [mGy]			Contrib. E [mSv]
	Clinical data	Preclinical data	IP fluid	Circulation	Sum	
Breasts	20		0.10	0.06	0.15	48
Colon		33	1.31	0.10	1.41	79
Lungs	130	(150)	0.34	0.09	0.44	312
RBM	30		0.54	0.07	0.61	72
Stomach		192	1.39	0.10	1.49	461
Liver	50	(31)	1.25	0.09	1.34	40
Oesophagus	55				0.08	44
Thyroid	595	(977)	0.01	0.07	0.08	476
Urine Bladder	276		0.91	0.10	1.01	221
Bone surfaces	55		0.70	0.22	0.92	11
Brain	55		<0.01	0.08	0.08	11
Salivary glands		180			0.08	36
Skin	55		0.08	0.04	0.12	11
Adrenals			1.95	0.10	2.05	
Gall bladder				0.10		
Heart	70	(60)	0.87	0.10	0.97	
Kidneys	84	(97)	1.42	0.09	1.51	
Pancreas			5.64	0.11	5.74	132
Muscle		18	0.49	0.07	0.57	
Small intestine		45	2.33	0.10	2.43	
Spleen		58	0.72	0.09	0.82	
Thymus			0.12	0.09	0.21	

5.2 Preclinical results

In Paper II, the effects of α -irradiation of the peritoneum were studied in a mouse model. Groups of mice were irradiated intraperitoneally by IP administration of ^{211}At -trastuzumab. Absorbed doses to the peritoneum delivered were around 0, 17.5, 35 and 50 Gy for the respective groups. The irradiation resulted in a dose-dependent general toxicity resulting in weight loss and premature death, see Figure 9.

No differences between irradiated and unirradiated mice were found upon macroscopical examination of the peritoneum, nor by immunohistochemical analysis of peritoneal membrane biopsies. This suggests that the poor health observed in irradiated animals had other causes than inflammation or irritation of the peritoneum. Peritoneal clearance measurements, however, indicated a moderate dose-dependent decrease in the peritoneal transport capacity, see Figure 8

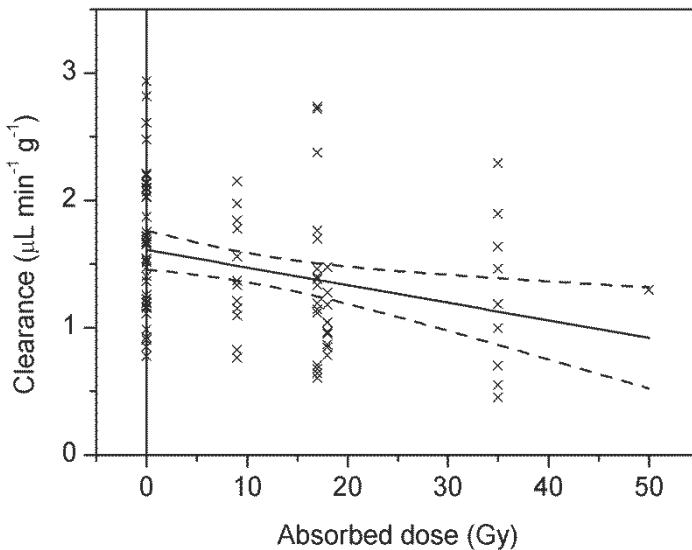


Figure 8 Peritoneal clearance rates in mice exposed to increasing absorbed doses to the peritoneum by IP injection of ^{211}At -trastuzumab.

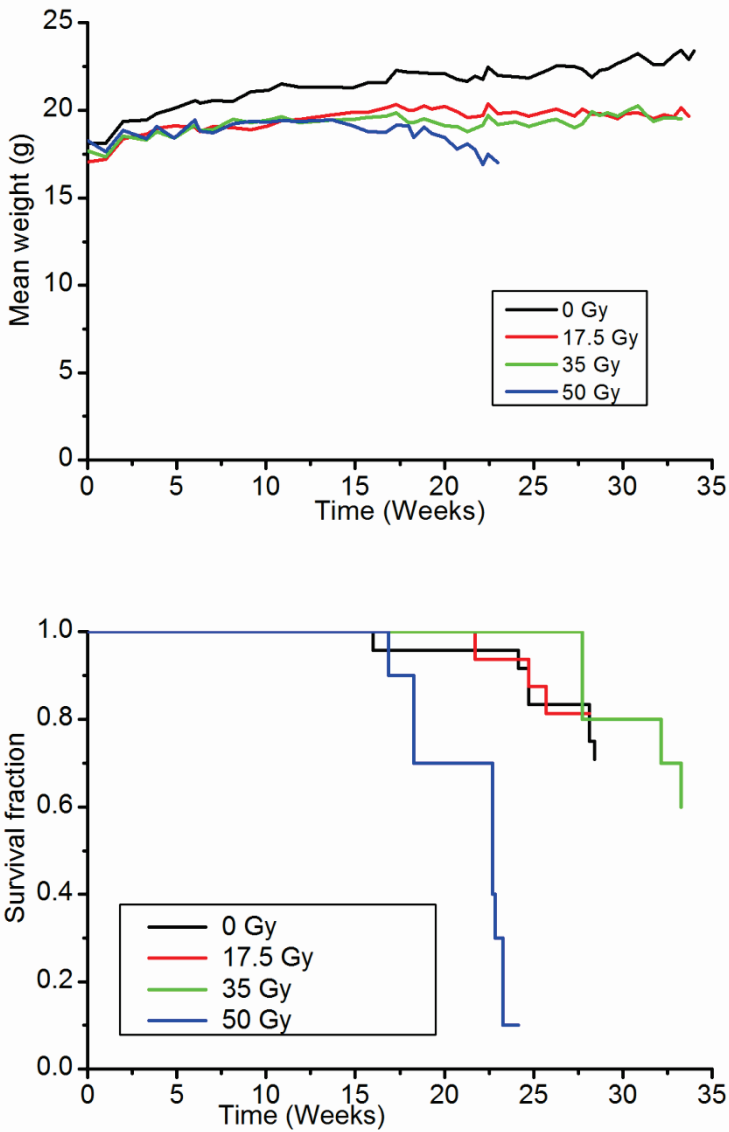


Figure 9 The mean body weight (upper) and a Kaplan-Meier plot showing the survival(lower) of mice exposed to increasing absorbed doses to the peritoneum by IP injection of ^{211}At -trastuzumab.

6 DISCUSSION AND CONCLUSIONS

The studies performed within the frame of this thesis, with support from several other publications from our research group [36, 37, 52, 56, 74, 115, 130-134], show that IP ^{211}At -RIT may become a promising new option for ovarian cancer patients. Although not specifically evaluated in patients, therapeutic absorbed doses can be delivered to intraperitoneally confined tumor cells with very low risk for acute side effects. With appropriate medication for blocking the uptake of free ^{211}At in normal organs, the tissue exposed to the highest absorbed dose during IP ^{211}At -RIT is the peritoneum on which the targeted cancer cells grow. The peritoneal absorbed dose level in question seems however to be well tolerated by patients and mice. The moderately reduced peritoneal transport capacity observed in mice appeared at higher absorbed dose levels than patients have been subjected to and there was no evidence that the other side effects observed in mice were of peritoneal origin. Rather, the difference in growth and survival observed between study groups in Paper II could be attributable to general radiation toxicity. Unfortunately, the high ratio between peritoneal and extra-peritoneal exposure found in humans was difficult to mimic in a mouse experiment with ^{211}At due to the relatively fast resorption rate of IP fluid in mice, which led to a high whole body irradiation in the mice. Therefore, the maximum tolerable absorbed dose to the peritoneum was not determined.

In paper I and III, the initial activity concentration of the IP infusate was chosen for normalization of pharmacokinetic data and absorbed doses instead of the more conventionally used amount of administered activity, with a few exceptions. The foremost reason for doing so was because the transport of radioimmunoconjugate from the peritoneal cavity to blood goes mainly via lymphatic drainage of the peritoneal cavity, a relatively steady flow of 27 ml min^{-1} [135]. Transport of radioimmunoconjugate to blood may thus be seen as a slow infusion over 24 h, after which the remaining IP fluid is evacuated. Since the volumetric flow is constant and only a small fraction of the total IP fluid volume passes over to blood, the amount of activity leaving the peritoneal cavity is determined by the concentration, not by the total amount of activity or by the IP infusion volume. Consequently, the absorbed doses to normal tissues outside of the peritoneal cavity, as well as to the peritoneum and targeted tumor cells, are proportional to the activity concentration of the IP infusate. Even if the IP fluid would not be evacuated, the argument would still hold considering the relatively short half-life of ^{211}At in relation to the slow transport rate; 90% of the initial activity has decayed by the time of evacuation. However, the variability of normalized data was of the same

magnitude irrespectively of normalization to amount or concentration, which might be explained by the small number of patients evaluated and the generally high level of uncertainty.

The therapy under evaluation in this thesis is suggested as an upfront addition to the standard treatment of ovarian cancer, which today is about 30% curative. There is currently no way of discriminating between patients as to whom is cured for life and whom will recur after a successful primary treatment. Hopes are that with the addition of IP ^{211}At -RIT the fraction of fully cured patients will increase. Hence, a group of already cured patients and patients with a chance of long survival are the target group for the suggested therapy. In this situation, the risk for inducing secondary disease with the additional treatment needs to be addressed, particularly since the risk associated with α -particle irradiation is considered high. Clinical experience with α -emitters is however very limited and the long term consequences are not well known. The effective dose provides a tool for assessment of risk for stochastic effects caused by irradiation [41]. Indeed, the data used in the calculations of Paper III had varying levels of uncertainty depending on the method used for acquisition. Care was however taken that none of the contributions to the effective dose should be underestimated. For instance, the preclinical biodistribution data used for dosimetry on organs which were not possible to evaluate from clinical material, were taken from a study where no blocking agent was used, which may be considered a worst case scenario. The result of the effective dose estimation was therefore expressed as a maximum value of which we can be relatively certain. But, one problem with applying the concept of the effective dose to IP ^{211}At -RIT is that the peritoneum, which is exposed to the highest absorbed dose of all normal tissues studied, is not included in the definition of the effective dose. The risk for long term complications in relation to the peritoneum, i.e., mesothelioma, is thus not accounted for in the value < 2 Sv.

The largest contributors to the effective dose were the thyroid, the stomach, the lungs and the urine bladder. There may be cause to optimize the therapy to reduce absorbed doses to these organs. Successful efforts have already been made to limit the uptake in the thyroid. The data suggests however that there may be room for improvement. The dosage and schema for administration of the blocking agent has not been evaluated. The stomach contribution was calculated from unblocked animal data and may thus be significantly overestimated. KClO_4 has been shown to have a good blocking effect on the stomach in preclinical studies [77, 136]. The uptake in lungs was estimated from SPECT images of low quality due to low count rate. The estimated absorbed dose (from α -particles), 130 mGy, however corresponded

surprisingly well with the absorbed dose estimated from preclinical biodistribution data, 150 mGy. Treatment with cysteine or thiocyanate ions may reduce the uptake of ^{211}At in the lungs [77] and reduce the effective dose. With effective blocking of accumulation sites, free ^{211}At is found in higher concentration in blood and will consequently be filtered by the kidneys to a greater extent, which is positive in the sense that the activity is excreted and will no longer contribute to irradiation of normal tissues. Increased irradiation of the urine bladder is the downside, but that may not be an issue. Simple adjustments to the clinical protocol such as encouraging a large intake of fluids and frequent urination during the therapy would reduce the absorbed dose to the urine bladder. Should this not lead to satisfactory results, treatment with diurethics or temporary inlay of a urinary catheter may be options to consider.

The risks associated with IP ^{211}At -RIT may to some extent be predicted by these calculations. For a gender-mixed working age population, exposure to 2 Sv corresponds to a risk increase for lethal cancer of about 8% [41]. The target group for the suggested therapy is however middle-aged to elderly women who, in most cases, have had their reproductive organs removed because of their primary disease. It is reasonable to assume that the risk increase would be lower for this group. To value these risks is however very difficult without knowledge of the efficacy of the treatment, the impact the therapy may have on patients' lives.

A common routine in therapeutic nuclear medicine is to administer a tracer substance, similar to the therapeutic drug, to study the pharmacokinetics in individual patients before giving the therapy. This is of particular importance if the amount of administered activity must be limited to avoid acute toxicity. In the phase I study, the absorbed doses estimated were all well below known tolerance levels. No dose limiting organ could be identified. Although the therapeutic efficacy has not yet been evaluated in patients, preclinical results indicate that the activity concentrations used on patients No. 10-12 were at a level where a good therapeutic effect could be expected and that further dose escalation may not significantly improve the outcome [137, 138]. Therefore, dose planning or patient-specific dosage may not be necessary in IP ^{211}At -RIT.

Continued monitoring of pharmacokinetics in ^{211}At -RIT patients and calculation of absorbed doses would however be very valuable [139]. As already stated, the consequences of exposure to α -particle irradiation are not fully understood. Weighting factors for tissue sensitivity and radiation quality are constantly under scrutiny. For instance, Priest et al. conclude that the α -

particle radiation sensitivity is tissue-dependent and that the use of a single radiation weighting factor is inconsistent with experimental results [140]. A new definition of RBE was furthermore recently suggested [141]. We therefore argue that absorbed doses to as many organs as possible should be estimated in all patients undergoing ^{211}At -RIT to provide a basis for future risk assessments. New tools for analyzing the pharmacokinetics in patients need to be developed to reduce the uncertainty of these estimations. In particular, a new protocol for ^{211}At -SPECT imaging, optimized for quantification, would be valuable. Development of a pharmacokinetic model for the transport of ^{211}At -mAb and free ^{211}At in the body would also be very valuable.

Clinical data might however never provide information on the microscopic distribution within organs, which for α -emitters in particular may strongly influence the biologic effect on the organ or organism scale [142]. Low mean absorbed doses on the organ level may hide high uptake in subpopulations of cells within an organ. Awareness of the importance of the small scale distribution within tumors and normal tissues is currently growing and tools for studying the effects are emerging. In addition to microdosimetric models being developed for different organs, e.g., the thyroid [143], Bäck and Jacobsson developed a technique for imaging the small scale distribution of an α -emitter in sectioned biopsies, the α -camera, with which it has been shown that factors such as the size, charge and affinity of the carrier molecule influence the intra-organ distribution and consequently the absorbed dose rates to organ and tumor substructures [128]. α -camera images may be used for dosimetric calculations directly or provide input data to pharmacokinetic models for dosimetry. The combination of preclinical studies, computational modelling and clinical experience will certainly lead to a better understanding of the biologic response to α -particle irradiation.

7 FUTURE PERSPECTIVES

The work presented in this thesis is part of a translational project ranging from development of new targeting agents, to radiochemistry, to preclinical and clinical studies. The next big step in this project is to evaluate the pharmacokinetics of ^{211}At -labeled RebmAb200, the humanized version of MX35, in ovarian cancer patients. The process of acquiring approval for such a study is currently underway. If results are positive, continued clinical trial of IP ^{211}At -RIT for ovarian cancer is anticipated.

In preparation of that study and for the further development of α -RIT in general a number of smaller projects are underway in our research group. For example, the possibility to optimize the ^{211}At -SPECT imaging protocol for improved quantitative accuracy will be investigated. A pharmacokinetic model for IP ^{211}At -RIT is under development which may give an improved understanding of the pharmacokinetics involved and provide a useful tool for dosimetric calculations. The long term effects of low doses of ^{211}At will be investigated in mice; the specific endpoints to be studied are currently being discussed. Module radiochemistry is being developed with the aim to achieve a closed system for the distillation of ^{211}At , radiolabeling and purification of radiopharmaceutical. Evaluation of the small scale distribution of ^{211}At -mAbs in excised normal tissues and tumors will continually be investigated by means of the α -camera technique with the aim to identify possible organs at risk and to optimize the therapy. The choice and schema for administration of blocking agent may be investigated in patients or preclinically. In parallel, the potential for ^{211}At -RIT of other malignancies such as prostate and breast cancer are being investigated. The possibility for combining ^{211}At -RIT with another radionuclide, such as ^{177}Lu or ^{131}I , may be investigated with the aim to treat larger tumors. The α -emitter ^{213}Bi is another interesting candidate for similar applications, the potential of which is also under investigation. Certainly, the experience acquired from the development of ^{211}At -RIT for ovarian cancer will benefit the development of other α -RIT applications.

ACKNOWLEDGEMENT

My main supervisor **Lars Jacobsson** has provided endless support and encouragement. Thank you Lars for everything! You made this possible. Your scientific expertise and your kind and caring guidance helped me surpass my own expectations by far. You are my mentor and role model.

My assistant supervisor **Ragnar Hultborn**, thank you for counseling on clinical topics and for always being positive and inspiring.

My assistant supervisor **Stig Palm** came in as my supervisor at closing time, but has nevertheless been an excellent support.

Special thanks to **Tom Bäck** for everything from hands on experimental work to constructive criticism and insightful thoughts shared. Although you have not been a formal supervisor, this work would certainly not have been possible without you.

Thanks to **Helena Kahu** for excellent help with animal experiments and especially for being a good friend at work. The hours spent in the lab with you were some of the best.

Former and current members of the Targeted Alpha Therapy Group, **Sture Lindegren, Sofia Frost, Jörgen Elgqvist, Anna Gustafsson, Emma Aneheim, Nicolas Chouin, Koshin Washiyama, Håkan Andersson, Per Albertsson, Kecke Elmroth, Kristina Claesson and Karin Magnander**, thank you all for good collaboration.

Thanks to Head of Department **Eva Forssell Aronsson** for giving me the opportunity to do my Ph.D. at the Department of Radiation Physics and for your support. I highly appreciate it.

Thanks to **Gunilla Adielsson** for administrative support and for being a good friend.

Thanks to all my other colleagues at GU and Sahlgrenska for the many long coffee breaks. Special thanks to **Maria Larsson, Johanna Dalmo, Anders Josefsson, Jenny Nilsson, Sara Asplund, Nils Rudqvist, Emilia Runge, Jeanette Ragnarsson** for being there.

Thanks to **Holger Jensen** at the PET and Cyclotron Unit, Rigshospitalet, Copenhagen, Denmark for providing the exclusive radionuclide ^{211}At .

Thanks to the group at the Department of Surgery: **Eva Angenete**, **Peter Falk** and **Marie-Louise Ivarsson** for a nice collaboration on paper II.

Thanks to my former mentors for inspiration and encouragement. Thank you, **Ingela Ahlstedt**, I feel so fortunate to have had you as my very first school teacher. You provided some useful mind tools I still use today. Thank you, **Eva Linde**, for a solid foundation in chemistry and math and for telling me what to do when there were too many good options. Special thanks to **Marianne Pollard** for support way beyond the call of duty. My life would have been a lot different without your guidance. I miss you my friend.

Thanks to my parents **Lars** and **Viviann Haglund** for everything you have done for me. Thanks also to my in-laws **Håkan** and **IngMarie Cedercrantz** for always being there for us.

Extra super special thanks to my husband **Daniel Cederkrantz** for all your love and support, for being my best friend, for the good life that we share and for your faith in me. The sky is the limit. Thanks also to my son **Vidar** for unconditional love and joy. You will always be my No. 1.

Thanks also to everyone that I forgot to mention. Please forgive me.

REFERENCES

1. Sawin, C.T. and D.V. Becker, *Radioiodine and the treatment of hyperthyroidism: the early history*. Thyroid, 1997. **7**(2): p. 163-76.
2. Strebhardt, K. and A. Ullrich, *Paul Ehrlich's magic bullet concept: 100 years of progress*. Nat Rev Cancer, 2008. **8**(6): p. 473-480.
3. Kirkwood, J.M., et al., *Immunotherapy of cancer in 2012*. CA Cancer J Clin, 2012. **62**(5): p. 309-35.
4. Newsome, B.W. and M.S. Ernstoff, *The clinical pharmacology of therapeutic monoclonal antibodies in the treatment of malignancy; have the magic bullets arrived?* Br J Clin Pharmacol, 2008. **66**(1): p. 6-19.
5. Wiseman, G.A. and T.E. Witzig, *Yttrium-90 (90Y) ibritumomab tiuxetan (Zevalin) induces long-term durable responses in patients with relapsed or refractory B-Cell non-Hodgkin's lymphoma*. Cancer biotherapy & radiopharmaceuticals, 2005. **20**(2): p. 185-8.
6. Vose, J.M., *Bexxar: novel radioimmunotherapy for the treatment of low-grade and transformed low-grade non-Hodgkin's lymphoma*. The Oncologist, 2004. **9**(2): p. 160-72.
7. Knox, S.J. and R.F. Meredith, *Clinical radioimmunotherapy*. Semin Radiat Oncol, 2000. **10**(2): p. 73-93.
8. Macklis, R.M., *Clinical Radioimmunotherapy and Systemic Targeted Radiopharmaceutical Therapy (STaRT) programs in a radiation oncology environment*. Am J Clin Oncol, 2006. **29**(6): p. 543-7.
9. Meredith, R.F., et al., *Brief overview of preclinical and clinical studies in the development of intraperitoneal radioimmunotherapy for ovarian cancer*. Clin Cancer Res, 2007. **13**(18 Pt 2): p. 5643s-5645s.
10. Pouget, J.P., et al., *Clinical radioimmunotherapy--the role of radiobiology*. Nat Rev Clin Oncol, 2011. **8**(12): p. 720-34.
11. Jain, M., et al., *Emerging trends for radioimmunotherapy in solid tumors*. Cancer Biother Radiopharm, 2013. **28**(9): p. 639-50.
12. Gopal, A.K., et al., *131I anti-CD45 radioimmunotherapy effectively targets and treats T-cell non-Hodgkin lymphoma*. Blood, 2009. **113**(23): p. 5905-10.
13. Rao, A.V., G. Akabani, and D.A. Rizzieri, *Radioimmunotherapy for Non-Hodgkin's Lymphoma*. Clin Med Res, 2005. **3**(3): p. 157-65.
14. Coliva, A., et al., *90Y Labeling of monoclonal antibody MOv18 and preclinical validation for radioimmunotherapy of human ovarian carcinomas*. Cancer Immunol Immunother, 2005. **54**(12): p. 1200-13.
15. Smith-Jones, P.M., et al., *Preclinical radioimmunotargeting of folate receptor alpha using the monoclonal antibody conjugate DOTA-MORAb-003*. Nucl Med Biol, 2008. **35**(3): p. 343-51.

16. Zacchetti, A., et al., *(177)Lu- labeled MOv18 as compared to (131)I- or (90)Y-labeled MOv18 has the better therapeutic effect in eradication of alpha folate receptor-expressing tumor xenografts.* Nucl Med Biol, 2009. **36**(7): p. 759-70.
17. Gryshkova, V., et al., *The study of phosphate transporter NAPI2B expression in different histological types of epithelial ovarian cancer.* Experimental oncology, 2009. **31**(1): p. 37-42.
18. Soares, I.C., et al., *In silico analysis and immunohistochemical characterization of NaPi2b protein expression in ovarian carcinoma with monoclonal antibody Mx35.* Applied immunohistochemistry & molecular morphology : AIMM / official publication of the Society for Applied Immunohistochemistry, 2012. **20**(2): p. 165-72.
19. Yin, B.W., et al., *Monoclonal antibody MX35 detects the membrane transporter NaPi2b (SLC34A2) in human carcinomas.* Cancer Immun, 2008. **8**: p. 3.
20. Heyerdahl, H., et al., *Targeted alpha therapy with 227Th-trastuzumab of intraperitoneal ovarian cancer in nude mice.* Curr Radiopharm, 2013. **6**(2): p. 106-16.
21. Milenic, D.E., et al., *Targeting HER2: a report on the in vitro and in vivo pre-clinical data supporting trastuzumab as a radioimmunoconjugate for clinical trials.* MAbs, 2010. **2**(5): p. 550-64.
22. Behring, E. and S. Kitasato, *Über das Zustandenkommen der Diphtherie-Immunität und der Tetanus-Immunität bei Tieren.* Dtsch. Med. Wschr., 1890. **16**: p. 1113-1114.
23. Kohler, G. and C. Milstein, *Continuous cultures of fused cells secreting antibody of predefined specificity.* Nature, 1975. **256**(5517): p. 495-7.
24. Porter, R.R., *The hydrolysis of rabbit γ -globulin and antibodies with crystalline papain.* Biochem J, 1959. **73**: p. 119-26.
25. Lachmann, P.J., *The purification of specific antibody as F(ab')₂ by the pepsin digestion of antigen-antibody precipitates, and its application to immunoglobulin and complement antigens.* Immunochemistry, 1971. **8**(1): p. 81-8.
26. Jones, R.G. and J. Landon, *A protocol for 'enhanced pepsin digestion': a step by step method for obtaining pure antibody fragments in high yield from serum.* J Immunol Methods, 2003. **275**(1-2): p. 239-50.
27. von Pawel-Rammingen, U., B.P. Johansson, and L. Bjorck, *IdeS, a novel streptococcal cysteine proteinase with unique specificity for immunoglobulin G.* EMBO J, 2002. **21**(7): p. 1607-15.
28. Yoshitake, S., et al., *Conjugation of glucose oxidase from Aspergillus niger and rabbit antibodies using N-hydroxysuccinimide ester of N-(4-carboxycyclohexylmethyl)-maleimide.* Eur J Biochem, 1979. **101**(2): p. 395-9.

29. Jain, R.K., *Physiological barriers to delivery of monoclonal antibodies and other macromolecules in tumors*. *Cancer Res*, 1990. **50**(3 Suppl): p. 814s-819s.
30. Nelson, A.L., *Antibody fragments: hope and hype*. *MAbs*, 2010. **2**(1): p. 77-83.
31. Vlasak, J. and R. Ionescu, *Fragmentation of monoclonal antibodies*. *MAbs*, 2011. **3**(3): p. 253-63.
32. Tjandra, J.J., L. Ramadi, and I.F. McKenzie, *Development of human anti-murine antibody (HAMA) response in patients*. *Immunol Cell Biol*, 1990. **68 (Pt 6)**: p. 367-76.
33. Roguska, M.A., et al., *Humanization of murine monoclonal antibodies through variable domain resurfacing*. *Proc Natl Acad Sci U S A*, 1994. **91**(3): p. 969-73.
34. Lopes dos Santos, M., et al., *Rebmab200, a humanized monoclonal antibody targeting the sodium phosphate transporter NaPi2b displays strong immune mediated cytotoxicity against cancer: a novel reagent for targeted antibody therapy of cancer*. *PLoS One*, 2013. **8**(7): p. e70332.
35. Franken, N.A., et al., *Comparison of RBE values of high-LET alpha-particles for the induction of DNA-DSBs, chromosome aberrations and cell reproductive death*. *Radiat Oncol*, 2011. **6**: p. 64.
36. Elgqvist, J., et al., *Myelotoxicity and RBE of ²¹¹At-conjugated monoclonal antibodies compared with ^{99m}Tc-conjugated monoclonal antibodies and ⁶⁰Co irradiation in nude mice*. *J Nucl Med*, 2005. **46**(3): p. 464-71.
37. Back, T., et al., *²¹¹At radioimmunotherapy of subcutaneous human ovarian cancer xenografts: Evaluation of relative biologic effectiveness of an alpha-emitter in vivo*. *J Nucl Med*, 2005. **46**(12): p. 2061-7.
38. Palm, S., et al., *In vitro effects of free ²¹¹At, ²¹¹At-albumin and ²¹¹At-monoclonal antibody compared to external photon irradiation on two human cancer cell lines*. *Anticancer Res*, 2000. **20**(2A): p. 1005-12.
39. Zyuzikov, N.A., et al., *The relationship between the RBE of alpha particles and the radiosensitivity of different mutations of Chinese hamster cells*. *Radiat Environ Biophys*, 2001. **40**(3): p. 243-8.
40. Claesson, K., et al., *RBE of alpha-particles from (²¹¹At) for complex DNA damage and cell survival in relation to cell cycle position*. *Int J Radiat Biol*, 2011. **87**(4): p. 372-84.
41. *The 2007 Recommendations of the International Commission on Radiological Protection. ICRP publication 103*. *Annals of the ICRP*, 2007. **37**(2-4): p. 1-332.
42. Alvarez, R.D., et al., *A Phase I study of combined modality (⁹⁰Yttrium-CC49 intraperitoneal radioimmunotherapy for ovarian cancer*. *Clin Cancer Res*, 2002. **8**(9): p. 2806-11.

43. Alvarez, R.D., et al., *Intraperitoneal radioimmunotherapy of ovarian cancer with 177Lu-CC49: a phase I/II study*. *Gynecol Oncol*, 1997. **65**(1): p. 94-101.
44. Crippa, F., et al., *Single-dose intraperitoneal radioimmunotherapy with the murine monoclonal antibody I-131 MOv18: Clinical results in patients with minimal residual disease of ovarian cancer*. *Eur J Cancer*, 1995. **31A**(5): p. 686-90.
45. Kramer, K., et al., *Phase I study of targeted radioimmunotherapy for leptomeningeal cancers using intra-Ommaya 131-I-3F8*. *J Clin Oncol*, 2007. **25**(34): p. 5465-70.
46. Meredith, R.F., et al., *Intraperitoneal radioimmunotherapy of ovarian cancer with lutetium-177-CC49*. *J Nucl Med*, 1996. **37**(9): p. 1491-6.
47. Muto, M.G., et al., *Intraperitoneal radioimmunotherapy of refractory ovarian carcinoma utilizing iodine-131-labeled monoclonal antibody OC125*. *Gynecol Oncol*, 1992. **45**(3): p. 265-72.
48. van Zanten-Przybysz, I., et al., *Radioimmunotherapy with intravenously administered 131I-labeled chimeric monoclonal antibody MOv18 in patients with ovarian cancer*. *J Nucl Med*, 2000. **41**(7): p. 1168-76.
49. Verheijen, R.H., et al., *Phase III trial of intraperitoneal therapy with yttrium-90-labeled HMFG1 murine monoclonal antibody in patients with epithelial ovarian cancer after a surgically defined complete remission*. *J Clin Oncol*, 2006. **24**(4): p. 571-8.
50. Bernhardt, P. and E. Forssell-Aronsson, *Estimation of metastatic cure after radionuclide therapy*. *Q J Nucl Med Mol Imaging*, 2007. **51**(4): p. 297-303.
51. Essler, M., et al., *Therapeutic efficacy and toxicity of (225)Ac-labelled vs. (213)Bi-labelled tumour-homing peptides in a preclinical mouse model of peritoneal carcinomatosis*. *EJNMMI*, 2012.
52. Elgqvist, J., et al., *Fractionated radioimmunotherapy of intraperitoneally growing ovarian cancer in nude mice with 211At-MX35 F(ab')₂: therapeutic efficacy and myelotoxicity*. *Nucl Med Biol*, 2006. **33**(8): p. 1065-72.
53. Song, H., et al., *Radioimmunotherapy of breast cancer metastases with alpha-particle emitter 225Ac: comparing efficacy with 213Bi and 90Y*. *Cancer Res*, 2009. **69**(23): p. 8941-8.
54. Meredith, R.F., et al., *Pharmacokinetics and Imaging of Pb-TCMC-Trastuzumab After Intraperitoneal Administration in Ovarian Cancer Patients*. *Cancer biotherapy & radiopharmaceuticals*, 2013.
55. McDevitt, M.R., et al., *Radioimmunotherapy with alpha-emitting nuclides*. *Eur J Nucl Med*, 1998. **25**(9): p. 1341-51.
56. Elgqvist, J., et al., *The Potential and Hurdles of Targeted Alpha Therapy - Clinical Trials and Beyond*. *Front Oncol*, 2014. **3**: p. 324.

57. McDevitt, M.R., et al., *An $^{225}\text{Ac}/^{213}\text{Bi}$ generator system for therapeutic clinical applications: construction and operation*. Appl Radiat Isot, 1999. **50**(5): p. 895-904.
58. Cordier, D., et al., *Targeted alpha-radionuclide therapy of functionally critically located gliomas with ^{213}Bi -DOTA-[Thi8, Met(O2)11]-substance P: a pilot trial*. Eur J Nucl Med Mol Imaging, 2010. **37**(7): p. 1335-44.
59. Morgenstern, A., F. Bruchertseifer, and C. Apostolidis, *Targeted alpha therapy with ^{213}Bi* . Curr Radiopharm, 2011. **4**(4): p. 295-305.
60. Sgouros, G., et al., *Pharmacokinetics and dosimetry of an alpha-particle emitter labeled antibody: ^{213}Bi -HuM195 (anti-CD33) in patients with leukemia*. J Nucl Med, 1999. **40**(11): p. 1935-46.
61. Cherel, M., et al., *^{213}Bi radioimmunotherapy with an anti-mCD138 monoclonal antibody in a murine model of multiple myeloma*. J Nucl Med, 2013. **54**(9): p. 1597-604.
62. Dadachova, E., et al., *Pre-clinical evaluation of a ^{213}Bi -labeled 2556 antibody to HIV-1 gp41 glycoprotein in HIV-1 mouse models as a reagent for HIV eradication*. PLoS One, 2012. **7**(3): p. e31866.
63. Gustafsson, A.M., et al., *Comparison of therapeutic efficacy and biodistribution of ^{213}Bi - and ^{211}At -labeled monoclonal antibody MX35 in an ovarian cancer model*. Nucl Med Biol, 2012. **39**(1): p. 15-22.
64. Song, H., et al., *^{213}Bi (alpha-emitter)-antibody targeting of breast cancer metastases in the neu-N transgenic mouse model*. Cancer Res, 2008. **68**(10): p. 3873-80.
65. Wilbur, D.S., et al., *Streptavidin in antibody pretargeting. 5. chemical modification of recombinant streptavidin for labeling with the alpha-particle-emitting radionuclides ^{213}Bi and ^{211}At* . Bioconjug Chem, 2008. **19**(1): p. 158-70.
66. Abbas, N., et al., *Experimental alpha-particle radioimmunotherapy of breast cancer using ^{227}Th -labeled p-benzyl-DOTA-trastuzumab*. EJNMMI Res, 2011. **1**(1): p. 18.
67. Melhus, K.B., et al., *Evaluation of the binding of radiolabeled rituximab to CD20-positive lymphoma cells: an in vitro feasibility study concerning low-dose-rate radioimmunotherapy with the alpha-emitter ^{227}Th* . Cancer Biother Radiopharm, 2007. **22**(4): p. 469-79.
68. Washiyama, K., et al., *^{227}Th -EDTMP: a potential therapeutic agent for bone metastasis*. Nucl Med Biol, 2004. **31**(7): p. 901-8.
69. Colletti, P.M., *New treatment option: ^{223}Ra chloride, the first approved unsealed alpha-emitting radiopharmaceutical*. Clin Nucl Med, 2013. **38**(9): p. 724-5.
70. Zalutsky, M.R., et al., *Clinical experience with alpha-particle emitting ^{211}At : treatment of recurrent brain tumor patients with ^{211}At -labeled chimeric antitenascin monoclonal antibody 81C6*. J Nucl Med, 2008. **49**(1): p. 30-8.

71. Andersson, H., et al., *The curative and palliative potential of the monoclonal antibody MOv18 labelled with 211At in nude mice with intraperitoneally growing ovarian cancer xenografts--a long-term study*. Acta Oncol, 2000. **39**(6): p. 741-5.
72. Andersson, H., et al., *Radioimmunotherapy of nude mice with intraperitoneally growing ovarian cancer xenograft utilizing 211At-labelled monoclonal antibody MOv18*. Anticancer Res, 2000. **20**(1A): p. 459-62.
73. Andersson, H., et al., *Comparison of the therapeutic efficacy of 211At- and 131I-labelled monoclonal antibody MOv18 in nude mice with intraperitoneal growth of human ovarian cancer*. Anticancer Res, 2001. **21**(1A): p. 409-12.
74. Back, T., et al., *Glomerular filtration rate after alpha-radioimmunotherapy with 211At-MX35-F(ab')₂: A long-term study of renal function in nude mice*. Cancer Biother Radiopharm, 2009. **24**(6): p. 649-58.
75. Garg, P.K., C.L. Harrison, and M.R. Zalutsky, *Comparative tissue distribution in mice of the alpha-emitter 211At and 131I as labels of a monoclonal antibody and F(ab')₂ fragment*. Cancer Res, 1990. **50**(12): p. 3514-20.
76. Larsen, R.H., et al., *Alpha-particle radiotherapy with 211At-labeled monodisperse polymer particles, 211At-labeled IgG proteins, and free 211At in a murine intraperitoneal tumor model*. Gynecol Oncol, 1995. **57**(1): p. 9-15.
77. Larsen, R.H., S. Slade, and M.R. Zalutsky, *Blocking [211At]astatide accumulation in normal tissues: preliminary evaluation of seven potential compounds*. Nucl Med Biol, 1998. **25**(4): p. 351-7.
78. McLendon, R.E., et al., *Radiotoxicity of systemically administered 211At-labeled human/mouse chimeric monoclonal antibody: a long-term survival study with histologic analysis*. Int J Radiat Oncol Biol Phys, 1999. **45**(2): p. 491-9.
79. Strickland, D.K., G. Vaidyanathan, and M.R. Zalutsky, *Cytotoxicity of alpha-particle-emitting m-[211At]astatobenzylguanidine on human neuroblastoma cells*. Cancer Res, 1994. **54**(20): p. 5414-9.
80. Zalutsky, M.R., et al., *Targeted alpha-particle radiotherapy with 211At-labeled monoclonal antibodies*. Nuclear Medicine and Biology, 2007. **34**(7): p. 779-85.
81. Akabani, G., et al., *In vitro cytotoxicity of 211At-labeled trastuzumab in human breast cancer cell lines: effect of specific activity and HER2 receptor heterogeneity on survival fraction*. Nucl Med Biol, 2006. **33**(3): p. 333-47.
82. Elgqvist, J., et al., *Intraperitoneal alpha-radioimmunotherapy in mice using different specific activities*. Cancer Biother Radiopharm, 2009. **24**(4): p. 509-13.

83. Supiot, S., et al., *Mechanisms of cell sensitization to alpha radioimmunotherapy by doxorubicin or paclitaxel in multiple myeloma cell lines*. Clin Cancer Res, 2005. **11**(19 Pt 2): p. 7047s-7052s.
84. Vallon, M., et al., *Enhanced efficacy of combined ²¹³Bi-DTPA-F3 and paclitaxel therapy of peritoneal carcinomatosis is mediated by enhanced induction of apoptosis and G2/M phase arrest*. Eur J Nucl Med Mol Imaging, 2012. **39**(12): p. 1886-97.
85. Yong, K.J., et al., *Sensitization of Tumor to Pb-212 Radioimmunotherapy by Gemcitabine Involves Initial Abrogation of G2 Arrest and Blocked DNA Damage Repair by Interference With Rad51*. International Journal of Radiation Oncology Biology Physics, 2013. **85**(4): p. 1119-1126.
86. Mueller, S., et al., *Cooperation of the HDAC inhibitor vorinostat and radiation in metastatic neuroblastoma: efficacy and underlying mechanisms*. Cancer Lett, 2011. **306**(2): p. 223-9.
87. Govindan, S.V., et al., *Use of galactosylated-streptavidin as a clearing agent with ¹¹¹In-labeled, biotinylated antibodies to enhance tumor/non-tumor localization ratios*. Cancer Biother Radiopharm, 2002. **17**(3): p. 307-16.
88. Bankhead, C.R., S.T. Kehoe, and J. Austoker, *Symptoms associated with diagnosis of ovarian cancer: a systematic review*. BJOG, 2005. **112**(7): p. 857-65.
89. Nelson, H.D., et al., *Genetic risk assessment and BRCA mutation testing for breast and ovarian cancer susceptibility: systematic evidence review for the U.S. Preventive Services Task Force*. Ann Intern Med, 2005. **143**(5): p. 362-79.
90. Whiteman, D.C., et al., *Timing of pregnancy and the risk of epithelial ovarian cancer*. Cancer Epidemiol Biomarkers Prev, 2003. **12**(1): p. 42-6.
91. Altman, A.D., et al., *Optimal debulking targets in women with advanced stage ovarian cancer: a retrospective study of immediate versus interval debulking surgery*. J Obstet Gynaecol Can, 2012. **34**(6): p. 558-66.
92. *Dödsorsaker 2007*. 2009, Sveriges officiella statistik, Hälso- och sjukvård.
93. Palm, S., et al., *Therapeutic efficacy of astatine-211-labeled trastuzumab on radioresistant SKOV-3 tumors in nude mice*. Int J Radiat Oncol Biol Phys, 2007. **69**(2): p. 572-9.
94. Elgqvist, J., et al., *Repeated Intraperitoneal alpha-Radioimmunotherapy of Ovarian Cancer in Mice*. J Oncol, 2010. **2010**: p. 394913.
95. Corson, D.R., K.R. MacKenzie, and E. Segrè, *Artificially Radioactive Element 85*. Physical Review, 1940. **58**(8): p. 672-678.

96. Guerard, F., J.F. Gestin, and M.W. Brechbiel, *Production of [(211)At]-Astatinated Radiopharmaceuticals and Applications in Targeted alpha-Particle Therapy*. Cancer biotherapy & radiopharmaceuticals, 2013. **28**(1): p. 1-20.
97. International Commission on Radiation Units and Measurements., *Stopping powers and ranges for protons and alpha particles*. ICRU report. 1993, Bethesda, Md., U.S.A.: International Commission on Radiation Units and Measurements. x, 286 p.
98. Larsen, R.H., B.W. Wieland, and M.R. Zalutsky, *Evaluation of an internal cyclotron target for the production of 211At via the 209Bi(alpha,2n)211 at reaction*. Appl Radiat Isot, 1996. **47**(2): p. 135-43.
99. Henriksen, G., et al., *Optimisation of cyclotron production parameters for the 209Bi(alpha, 2n) 211At reaction related to biomedical use of 211At*. Appl Radiat Isot, 2001. **54**(5): p. 839-44.
100. Lindegren, S., T. Back, and H.J. Jensen, *Dry-distillation of astatine-211 from irradiated bismuth targets: A time-saving procedure with high recovery yields*. Appl Radiat Isot, 2001. **55**(2): p. 157-60.
101. Mattes, M.J., et al., *Mouse monoclonal antibodies to human epithelial differentiation antigens expressed on the surface of ovarian carcinoma ascites cells*. Cancer Res, 1987. **47**(24 Pt 1): p. 6741-50.
102. Gryshkova, V., et al., *Generation of Monoclonal Antibodies Against Tumor-Associated Antigen MX35/sodium-Dependent Phosphate Transporter NaPi2b*. Hybridoma, 2011. **30**(1): p. 37-42.
103. Frei, P., et al., *Identification and localization of sodium-phosphate cotransporters in hepatocytes and cholangiocytes of rat liver*. American Journal of Physiology-Gastrointestinal and Liver Physiology, 2005. **288**(4): p. G771-G778.
104. Huber, K., A. Muscher, and G. Breves, *Sodium-dependent phosphate transport across the apical membrane of alveolar epithelium in caprine mammary gland*. Comparative Biochemistry and Physiology a-Molecular & Integrative Physiology, 2007. **146**(2): p. 215-222.
105. Traebert, M., et al., *Expression of type IINa-P-i cotransporter in alveolar type II cells*. American Journal of Physiology-Lung Cellular and Molecular Physiology, 1999. **277**(5): p. L868-L873.
106. Xu, Y.X., et al., *Sodium-inorganic phosphate cotransporter NaPi-IIb in the epididymis and its potential role in male fertility studied in a transgenic mouse model*. Biology of Reproduction, 2003. **69**(4): p. 1135-1141.
107. Homann, V., et al., *Sodium-phosphate cotransporter in human salivary glands: Molecular evidence for the involvement of NPT2b in acinar phosphate secretion and ductal phosphate reabsorption*. Archives of Oral Biology, 2005. **50**(9): p. 759-768.
108. Brollo, J., et al., *Adjuvant trastuzumab in elderly with HER-2 positive breast cancer: A systematic review of randomized controlled trials*. Cancer Treatment Reviews, 2013. **39**(1): p. 44-50.

109. Hudis, C.A., *Drug therapy: Trastuzumab - Mechanism of action and use in clinical practice*. New England Journal of Medicine, 2007. **357**(1): p. 39-51.
110. Abbas, N., et al., *Radioimmunotherapy of Mice with HER-2 Positive SKOV-3 Xenografts Using Th-227- and Lu-177-labeled p-benzyl-DOTA-trastuzumab*. European Journal of Nuclear Medicine and Molecular Imaging, 2010. **37**: p. S314-S314.
111. Abbas, N., et al., *Radioimmunotherapy of Mice with HER-2 Positive SKBR-3 Xenografts Using Th-227-p-benzyl-DOTA-trastuzumab*. European Journal of Nuclear Medicine and Molecular Imaging, 2010. **37**: p. S282-S283.
112. Rasaneh, S., et al., *Radioimmunotherapy of mice bearing breast tumors with Lu-177-labeled trastuzumab*. Turkish Journal of Medical Sciences, 2012. **42**: p. 1292-1298.
113. Rasaneh, S., et al., *Radiolabeling of trastuzumab with Lu-177 via DOTA, a new radiopharmaceutical for radioimmunotherapy of breast cancer*. Nuclear Medicine and Biology, 2009. **36**(4): p. 363-369.
114. Lindegren, S., et al., *High-efficiency astatination of antibodies using N-iodosuccinimide as the oxidising agent in labelling of N-succinimidyl 3-(trimethylstannyl)benzoate*. Nucl Med Biol, 2001. **28**(1): p. 33-9.
115. Lindegren, S., et al., *Direct procedure for the production of ²¹¹At-labeled antibodies with an epsilon-lysyl-3-(trimethylstannyl)benzamide immunoconjugate*. J Nucl Med, 2008. **49**(9): p. 1537-45.
116. Lindmo, T., et al., *Determination of the immunoreactive fraction of radiolabeled monoclonal antibodies by linear extrapolation to binding at infinite antigen excess*. J Immunol Methods, 1984. **72**(1): p. 77-89.
117. Shaw, T.J., et al., *Characterization of intraperitoneal, orthotopic, and metastatic xenograft models of human ovarian cancer*. Molecular Therapy, 2004. **10**(6): p. 1032-1042.
118. Hamilton, T.C., et al., *Characterization of a human ovarian carcinoma cell line (NIH:OVCAR-3) with androgen and estrogen receptors*. Cancer Res, 1983. **43**(11): p. 5379-89.
119. Turkington, T.G., et al., *Measuring astatine-211 distributions with SPECT*. Physics in Medicine and Biology, 1993. **38**(8): p. 1121-30.
120. Eckerman, K. and A. Endo, *ICRP Publication 107. Nuclear decay data for dosimetric calculations*. Ann ICRP, 2008. **38**(3): p. 7-96.
121. Msaki, P., et al., *Generalized scatter correction method in SPECT using point scatter distribution functions*. Journal of nuclear medicine : official publication, Society of Nuclear Medicine, 1987. **28**(12): p. 1861-9.

122. Msaki, P., B. Axelsson, and S.A. Larsson, *Some physical factors influencing the accuracy of convolution scatter correction in SPECT*. Physics in Medicine and Biology, 1989. **34**(3): p. 283-98.
123. Bolch, W.E., et al., *MIRD Pamphlet No. 21: A Generalized Schema for Radiopharmaceutical Dosimetry--Standardization of Nomenclature*. J Nucl Med, 2009. **50**(3): p. 477-484.
124. Stabin, M.G. and J.A. Siegel, *Physical models and dose factors for use in internal dose assessment*. Health Physics, 2003. **85**(3): p. 294-310.
125. Snyder, W.S., M.R. Ford, and J.W. Poston, *Tabulation of Dose Equivalent Per Microcurie-Day for Source and Target Organs of an Adult for Various Radionuclides*. Transactions of the American Nuclear Society, 1974. **18**(Jun23): p. 387-388.
126. Watson, E.E., et al., *A model of the peritoneal cavity for use in internal dosimetry*. Journal of nuclear medicine : official publication, Society of Nuclear Medicine, 1989. **30**(12): p. 2002-11.
127. Chu, S.Y.F., L.P. Ekström, and R.B. Firestone, *WWW Table of Radioactive Isotopes*. 1999.
128. Back, T. and L. Jacobsson, *The alpha-camera: a quantitative digital autoradiography technique using a charge-coupled device for ex vivo high-resolution bioimaging of alpha-particles*. Journal of nuclear medicine : official publication, Society of Nuclear Medicine, 2010. **51**(10): p. 1616-23.
129. Palm, S., et al., *Microdosimetry of astatine-211 single-cell irradiation: role of daughter polonium-211 diffusion*. Med Phys, 2004. **31**(2): p. 218-25.
130. Back, T.A., et al., *Tumor Growth of Subcutaneous Xenografts after Repeated Alpha-Radioimmunotherapy with Astatine-211: What Absorbed Dose is Required to Treat Solid Tumors with Alpha-particle Emitters?* European Journal of Nuclear Medicine and Molecular Imaging, 2012. **39**: p. S324-S324.
131. Chouin, N., et al., *Ex Vivo Activity Quantification in Micrometastases at the Cellular Scale Using the alpha-Camera Technique*. Journal of nuclear medicine : official publication, Society of Nuclear Medicine, 2013.
132. Andersson, H., et al., *Astatine-211-labeled antibodies for treatment of disseminated ovarian cancer: an overview of results in an ovarian tumor model*. Clin Cancer Res, 2003. **9**(10 Pt 2): p. 3914S-21S.
133. Chouin, N., et al., *Quantification of activity by alpha-camera imaging and small-scale dosimetry within ovarian carcinoma micrometastases treated with targeted alpha therapy*. The quarterly journal of nuclear medicine and molecular imaging : official publication of the Italian Association of Nuclear Medicine, 2012. **56**(6): p. 487-95.

134. Elgqvist, J., et al., *Administered activity and metastatic cure probability during radioimmunotherapy of ovarian cancer in nude mice with (211)At-MX35 F(ab')(2)*. Int J Radiat Oncol Biol Phys, 2006. **66**(4): p. 1228-37.
135. Moberly, J.B., et al., *Pharmacokinetics of icodextrin in peritoneal dialysis patients*. Kidney Int Suppl, 2002(81): p. S23-33.
136. Frost, S.H., et al., *In vivo distribution of avidin-conjugated MX35 and (211)At-labeled, biotinylated poly-L-lysine for pretargeted intraperitoneal alpha-radioimmunotherapy*. Cancer Biother Radiopharm, 2011. **26**(6): p. 727-36.
137. Elgqvist, J., et al., *Alpha-radioimmunotherapy of intraperitoneally growing OVCAR-3 tumors of variable dimensions: Outcome related to measured tumor size and mean absorbed dose*. J Nucl Med, 2006. **47**(8): p. 1342-50.
138. Elgqvist, J., et al., *Therapeutic efficacy and tumor dose estimations in radioimmunotherapy of intraperitoneally growing OVCAR-3 cells in nude mice with (211)At-labeled monoclonal antibody MX35*. J Nucl Med, 2005. **46**(11): p. 1907-15.
139. Palm, S., J. Elgqvist, and L. Jacobsson, *Patient-specific alpha-particle dosimetry*. Curr Radiopharm, 2011. **4**(4): p. 329-35.
140. Priest, N.D., D.G. Hoel, and P.N. Brooks, *Relative toxicity of (45)Ca beta-particles and (242)Cm alpha-particles following their intravenous injection into mice as radiolabelled FAP*. International Journal of Radiation Biology, 2010. **86**(4): p. 300-20.
141. Hobbs, R.F., et al., *Redefining Relative Biological Effectiveness in the Context of the EQDX Formalism: Implications for Alpha-Particle Emitter Therapy*. Radiat Res, 2014. **181**(1): p. 90-8.
142. Sgouros, G., R.F. Hobbs, and H. Song, *Modelling and dosimetry for alpha-particle therapy*. Curr Radiopharm, 2011. **4**(3): p. 261-5.
143. Josefsson, A. and E. Forssell-Aronsson, *Microdosimetric analysis of 211At in thyroid models for man, rat and mouse*. EJNMMI Res, 2012. **2**(1): p. 29.